The Influence of Paper Surface Chemistry on Bacteriophage Activity

The Influence of Paper Surface Chemistry on Bacteriophage Activity

By

JUNHAI LIN, B. Eng.

A Thesis

Submitted to the School of Graduate Studies

in Partial Fulfillment of the Requirements

for the Degree

Master of Applied Science

McMaster University

MASTER OF APPLIED SCIENCE (2008) McMaster University
(Chemical Engineering) Hamilton, Ontario

TITLE: The Influence of Paper Surface Chemistry on Bacteriophage Activity

AUTHOR: Junhai Lin, B. Eng (South China University of Technology)

SUPERVISOR: Dr. R.H. Pelton and Dr. C. Filipe

NUMBER OF PAGES: Xiii; 69

Abstract:

Bacteriophages are promising biosensing systems in bioactive paper application due to their specific detection of bacteria. Different chemicals including wet strength resins were used to improve paper properties. This work investigated the influence of wet strength resins (PAE and PVAm) on bacteriophage activity, and proposed another method of using PolyNIPAM microgel to separate bacteriophage from paper surface. Compared with filter paper, the cationic polymer PAE and PVAm treated paper exhibited high phage binding efficiency but low phage activity due to the electrostatic interaction. PVAm had strong phage adsorption and almost completely deactivated the phage particle. Streptavidin was coupled to PolyNIPAM microgel in the presence of EDC, and T4 bacteriophage genetically modified with biotin was immobilized to microgel particle which resulted in a 10-fold improvement in attachment when compared with T4 wild-type phage. The microgel-phage coupling efficiency was very low, there were more than 10^6 microgel particle for every active phage. And microgel supported phages were deactivated after coating on the PAE/PVAm treated paper.

Acknowledgements

First, I would like to thank my supervisors Dr. Robert Pelton and Dr. Carlos Filipe, for their valuable guidance and support through my graduate studies at McMaster. With their intelligence and encouragement, I not only learned scientific knowledge, but more importantly how to do research and give presentations.

I would like to thank Dr. Mansel Griffiths and Mona Tolba from University of Guelph for giving me the training of phage preparation and providing all the phage samples.

Special appreciation goes to Dr. Shunxing Su, for his kindness to assist me at the earlier stage of my project and the training of microgel preparation.

I am also sincerely grateful to all my colleagues, past and presents, in Robert Pelton's group: Lily, Ebenesio, Lucy, Wei, Yuguo, Chengming, Justin, Jerry, Miao, Lou, Tracy, Quan, Songtao, Jessie, Selina, Dan, Frances and Doug for their friendship, which made my life in McMaster very enjoyable and memorable.

I especially would like to thank my wife and parents for their endless love and support.

Finally, I want to thank SENTINEL bioactive paper network for providing the research funding.

Table of Contents:

List of Figures:

List of Tables:

Abbreviation:

AA	Acrylic Acid
APS	Ammonium persulfate
BSA	Bovine serum albumin
CBM	Cellulose binding modules
E. coli	*Escherichia coli*
EDC	1-Ethyl-3-(3-dimethylaminopropyl)-carbodiimide
IP	Isoelectric point
kbp	kilo base pair
LCST	Lower critical solution temperature
MAA	Methacrylic acid
MBA	N,N-Methylenebisacrylamide
MES	2-(N-morpholino) ethanesulfonic acid
NIPAM	N-isopropylacrylamide
PAAM	Polyallylamine
PAE	Polyamide-epichlorohydrin
Phage	Bacteriophage
PMAA	Poly(methacrylic acid)
PNVF	Poly(N-vinylformamide)
PS	Polystyrene
PVAm	Polyvinylamine
SP	Streptavidin
Sulfo-NHS	N-hydroxysulfosuccinimide
VAA	Vinylacetic acid
VPTT	Volume phase transition temperature

Chapter 1: Introduction

Over the past few years, due to events surrounding SARS, bird flu and tainted beef, the human health problem has drawn large amounts of attention and different methods have been investigated to detect pathogens. During the last several centuries, paper, which is inexpensive, disposable and sterile, has been widely used as sterile packaging, face masks and clothing, to protect human being from pathogens.[1] However, the application of the paper-based products is limited only as a passive barrier or filter. Thus, Dr. Pelton proposed the concept "bioactive paper", that is, paper that can detect, capture and deactivate water and airborne pathogens.[1]

One of the biggest challenges for bioactive paper is the development of inexpensive, highly sensitive and highly specific biosensing systems. Biosensors are defined as measurement devices that incorporate the biological entity to detect and quantify a specific event.[2] A typical biosensor consists of a receptor (polymer, enzyme, antibody, cell or micro-organism) and a transducer, which can transfer the change detected by the receptor into an understandable signal.[3] The standard method for detecting pathogens in drinking water and supplies, is the microbiological culture technique,[4] but it could take several days to grow the bacteria to the detection level. Enzyme-Linked Immunosorbent Assay (ELISA) is another conventional method of detecting pathogens, which involves the antibody-antigen interaction.[5] Polymerase

Chain Reaction (PCR) may also be used for simultaneous detection of the pathogens.[6] Nevertheless, these techniques still require higher level of bacteria growth for detection. Meanwhile, Fratamico et al. utilized the Surface Plasmon Resonance (SPR) to effectively detect the *Escherichia coli*(*E. coli*) bacteria.[7] However, this technique requires a high level of specificity and stability of the recognition agent, and antibodies have been frequently used in this system due to its specific interaction with antigen. However, apart from the fact that the antibody method is prone to being influenced by the environment, it is also labour-consuming and expensive in terms of its production, isolation and purification.[8]

Another promising probe for specific biosensing is bacteriophage (phage).[8] Phages are viruses, which can specifically detect the bacteria. This unique specificity provides significant chances for biosensor development. In terms of paper-based applications, the phages have to be covalently bound to the paper surfaces. However, directly binding the phages to the paper surfaces may not be a promising approach, due to the surface chemistry of the packaging and paper products. In order to enhance the dry/wet strength and reduce the liquid absorption, the paper surfaces have been treated with different chemicals.[9] Meanwhile, most of the applications for bioactive paper require wet conditions. Thus, the cationic wet strength resins, which can retain some of paper's original dry strength when wet, would be necessary for developing the bioactive paper. However, the biosensing property of the phages may be

significantly affected by the wet strength resins in terms of directly coupling, probably causing the phages to denature after binding. Moreover, the orientational attachment of phages to sensor surfaces may also improve the sensor performance, because phages detect target bacteria through functional receptors located at the phage tail positions.[10]

Thus, the objective of my project was to first investigate the influence of wet strength resin and treated paper on the phage activity. This lead to the development of a method to eliminate the possible influence of the paper surface chemistry on the phage activity, using carboxylated poly(N-isopropylacrylamide) (PolyNIPAM) microgels as the supporting materials to separate phages from the paper surface chemistry. Streptavidin-biotin complex was used to immobilize phage to the microgel particle.

Chapter 2: Literature review

2.1 Bacteriophage

Phages are viruses that only infect bacteria, and they have various sizes and shapes. They are one of the most abundant living entities in the world, and their estimated numbers reach 10^{30} to 10^{32} in total. Since their discovery in 1915, phages have been broadly studied worldwide, and used in different kinds of applications.[11]

2.1.1 Brief history of the phage research.

Phages were discovered by Frederick W. Twort in 1915. When he tried to grow *vaccinia virus* on the agar plate, he observed many colonies grew up on the plates, which he called "glass transformation".[11] Then, in 1917, Felix d'Herelle concluded that the invisible agents (phages) need living cells to multiply, and the plaque count could be a potential way to count the invisible agents.[12] Starting in 1940s, the newly invented electron microscope was used to visualize the phage and its infection of bacteria, meanwhile, the widespread use of antibiotics overshadowed the phage research.[13] Until 1980s, Smith and Huggins showed that phages can be more effective than antibiotics in aquaculture.[14] Since the 1990s, the biotech industry started applying the phage therapy in western countries. Now, the importance of phage is ever-increasing in western clinics due to the emergence of antibiotic-resistance bacteria.[13]

2.1.2 T4 phages

Figure 1 shows the structure of the T4 phage. The phage consists of a head (capsid), where the nucleic acid genome (DNA) is enclosed, and a tail. The tail has a shape of a hollow fiber, and at the end of the tail, there is a baseplate and several tail fibers, they are used to attach to the bacteria before injecting the DNA. The size of the phages range from 20nm to 200nm.

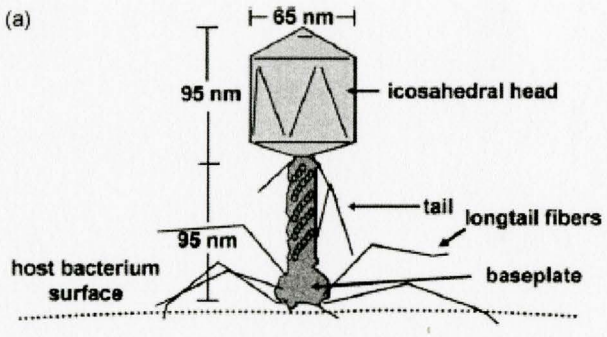

Figure 1: The structure of T4 bacteriophage (from ref 10)

The T4 phage has the largest size among all the phages, about 200nm long and 80-100 nm wide. Its DNA is 169 kbp (kilo base pair) long[11], also the longest among phages.[11] T4 phage is one of the most important and most thoroughly studied living entities in the world[11], due to its specific infection of *E. coli* bacteria. Figure 2 is the electron micrograph of phage.

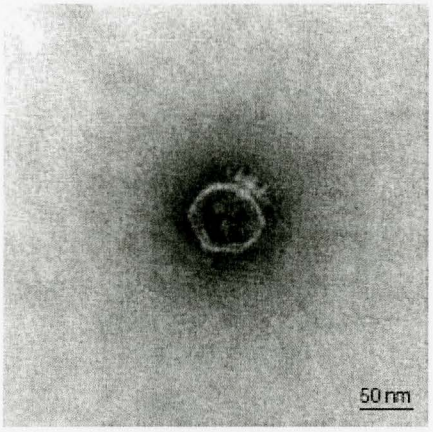

Figure 2: Electron micrograph of bacteriophage (from ref. 13)

2.1.3 Lytic replication of T4 bacteriophages

Figure 3 shows the five different stages of T4 bacteriophages replication cycle on *E. coli* bacteria: Attachment, Entry, Synthesis, Assembly and Release.

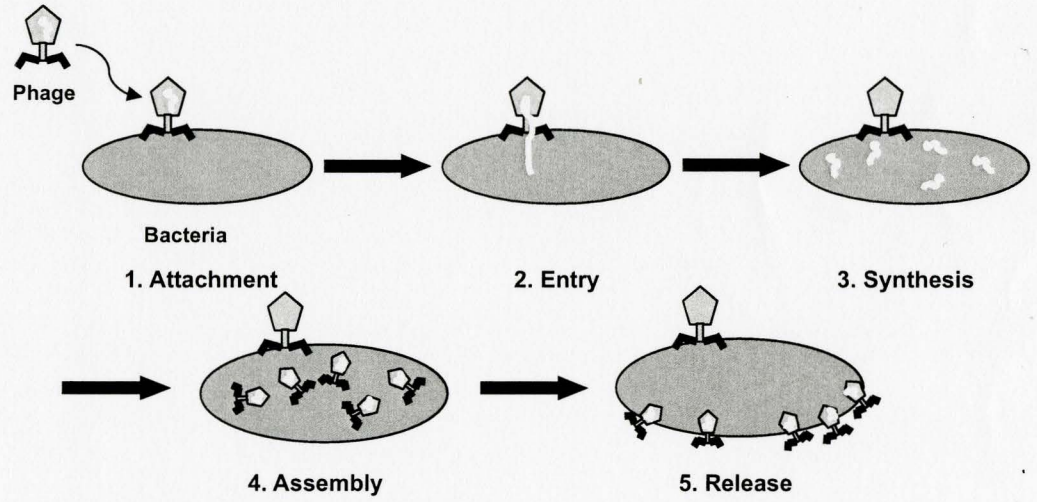

Figure 3: The replication cycle of T4 phage on *E. coli* bacteria.

Attachment happens precisely between proteins on T4 phages tail fibers and receptor proteins on the surface of the bacteria cell.[15] The specificity of attachment

determines that the T4 phages will only fit *E. coli* bacteria. After attachment, T4 phages release a protein carried on the capsid-*Lysozyme*, which can cross the peptidoglycan layer of the bacterial cell wall.[16] Then the phage genome moves into the bacteria through the hollow tube. After entry, the phage genome starts to synthesize the new phage proteins, including the head and tail capsomeres and lysozyme, and proceed to assemble into new host cells. Finally, the new assembled phages are released from the cell wall and the bacteria lyses. Figure 4 shows the T4 phage plaque in the bacterial lawn, the black spots are the areas where *E. coli* bacteria have been disintegrated. For T4 phage, the whole replication process can take about 25 minutes.[15]

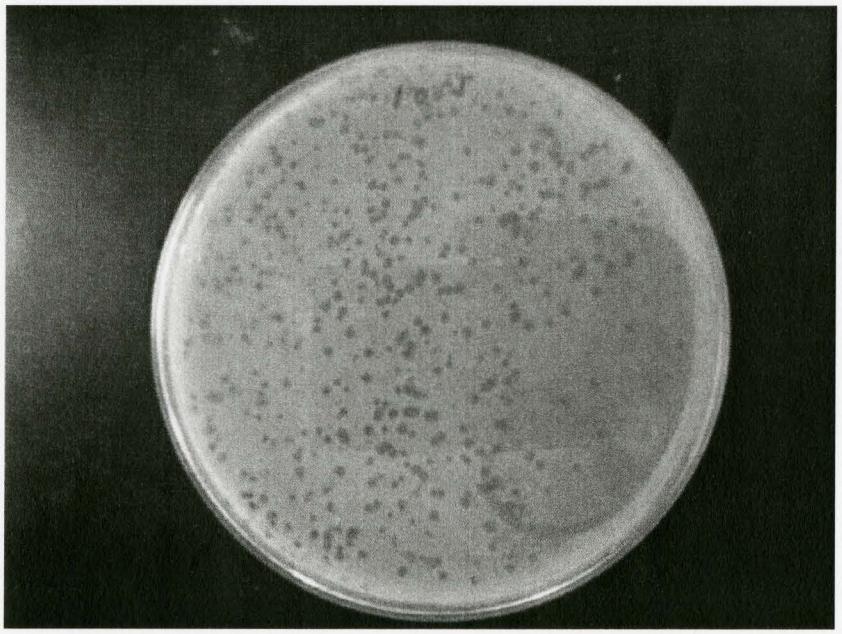

Figure 4: Phage plaque in the bacterial lawn on the surface of the agar plates

The specificity of the phages to unique bacteria opens a significant application to the biosensor system. However, random attachment of the phage onto biosensor surfaces would largely decrease activity of the phages (Figure 5).

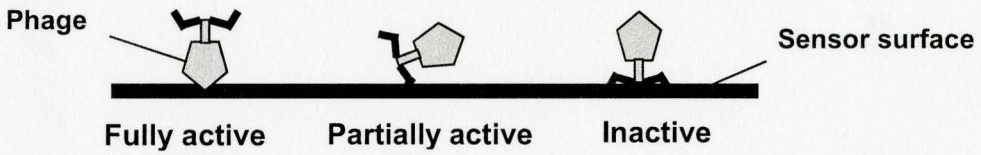

Figure 5: The random physical adsorption of phage onto biosensor surface.

Meanwhile, the chemical attachment (orientational attachment) of phages onto the sensor surfaces may substantially increase the activity. Sun et al. prepared the biotinylated-phage (biotin-phage) based biosorbent. In the experiment, the phage head protein had been biotinylated and the phage tail was left to attach to the bacteria. Their results showed a significant increase in attachment by phage-based biosorbent than by physical absorption.[17] Gervais et al. reported the streptavidin-mediated attachment of biotin-phage onto gold electrodes, and there was a 15-fold improvement in phage attachment onto gold electrode surfaces compared with wild type phage.[10]

2.2 *E. coli* bacteria

Bacteria are prokaryotic organism, and unlike the eukaryotes cells, the prokaryotic cells do not have a nucleus. The size of the bacteria cells are normally measured by micrometers, ranging from 1-10 μm. Historically, the bacteria has caused

some major diseases, however, the pathogenic bacteria only comprise a tiny portion of the entire family. Generally, many bacteria cause little harm and are useful for mankind. It is important to understand bacteria so as to effectively maximize its benefits and minimize its harmfulness.[18]

E. coli is one of the smallest and most understood bacteria. It has a rod-shaped cell, with a length of about 2.5μm (Figure 6). Like other bacteria, *E. coli* are the prokaryotic cells, which means they don't have a nucleus. *E. coli* is the most frequent species used in biotechnological research, due to its ease to grow and relatively simple structure.[19]

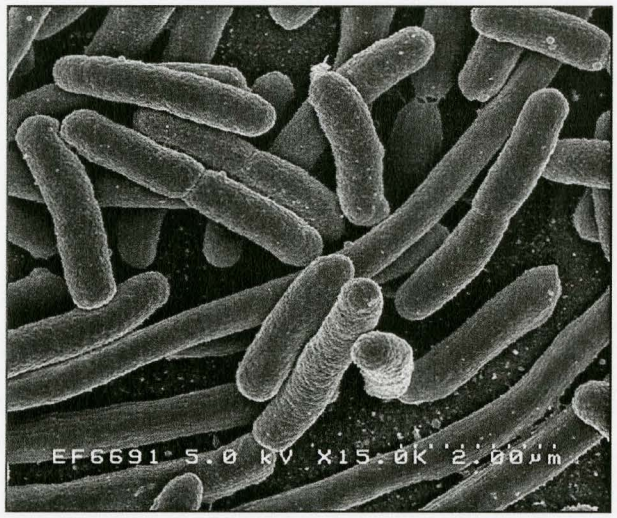

Figure 6: Structure of *E. coli* (from Rocky Mountain Laboratories, NIAID, NIH)

2.2.1 Growth of *E. coli* bacteria

The growth of *E. coli* bacteria refers to the increase of its population, resulting in a discrete colony. There are several crucial requirements for the growth, such as:

nutrients, energy, water, temperature and pH. Optimal growth temperature and pH for *E. coli* bacteria are 37°C and pH 6.5-7.5 (neutral).[18]

E. coli growth follows a pattern depicted by a cell cycle. The cell cycle refers to the process by which a living cell grows and divides into two cells. Most of the *E. coli* growth occurs in liquid media, where the progeny can move freely and disperse throughout the media. Figure 7 shows the typical growth curve of *E. coli* in LB medium at 37°C. There are four distinctive phases for the growth curve: the Lag Phase, the Log Phase, the Stationary Phase and Death Phase.[15] In the Lag Phase, most of the bacteria do not reproduce immediately, instead they are adjusting to the new medium environment; In the Log Phase, as its name indicates, the number of *E. coli* bacteria increase logarithmically, which could last for several hours. Then in the Stationary Phase, the number of dying cells equal to the number of new cells, and finally, the number of the cells start to decrease in the Death Phase.

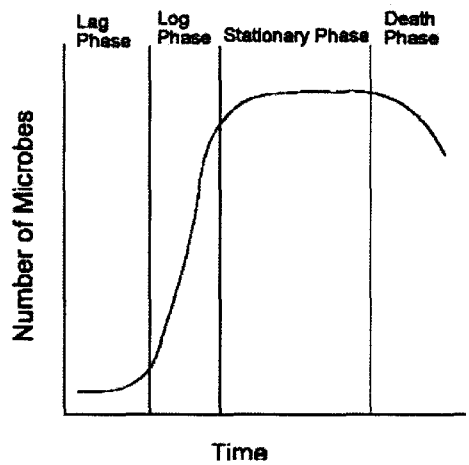

Figure 7: The growth curve of *E. coli* bacteria
(From http://www.eng.auburn.edu/~wfgale/usda_course/pasteur_page1.htm)

2.2.2 Measuring the bacterial number

Pour plate technique is one of the most popular methods used for measuring the bacterial number (Figure 8). CFU (Colony Forming Units) is employed as the units of the bacterial number. After culturing the *E. coli* bacteria, a series of 10-fold dilutions samples are made, and then poured onto agar plates. The number of *E. coli* bacteria can be counted after overnight incubation. The plates containing high concentration of *E. coli* could result in too many colonies to count. 30-300 colonies in an agar plates are the optimal countable number.[15]

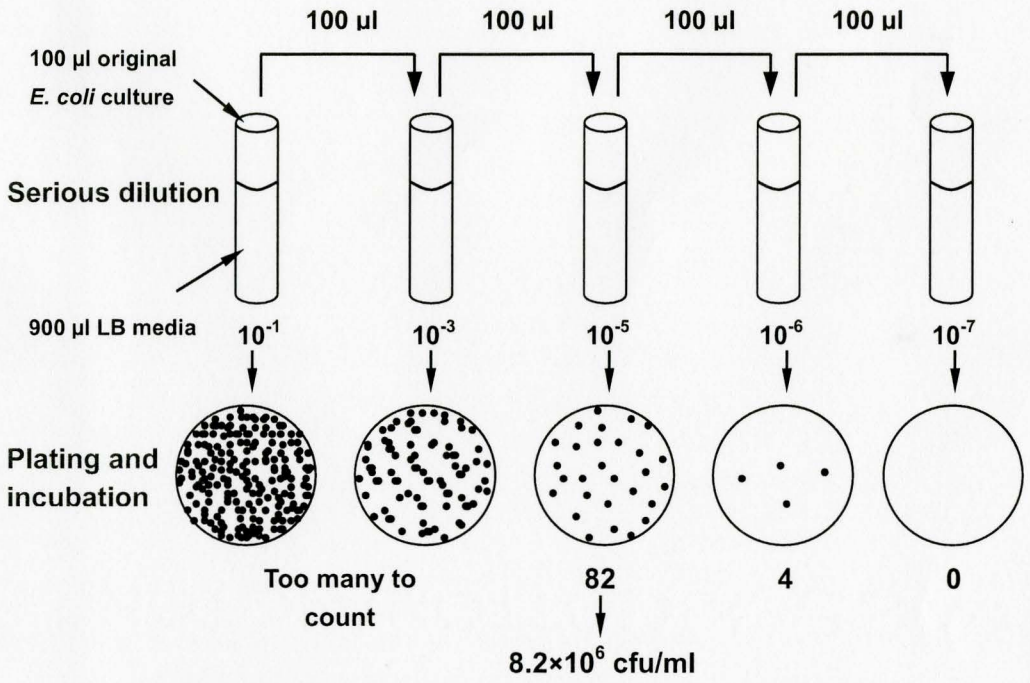

Figure 8: Pour plates count for estimating bacterial number.

2.3 Paper wet strength agent

When paper is wetted, its strength deteriorates because the water breaks its internal fiber bonding. In the papermaking industry, sizing is a process of paper chemical treatment in which the major objectives are: limiting the liquid absorption and increasing the dry/wet strength of the paper sheet.[9] Wet strength resins are usually water soluble, cationic polymers.[20] Once the resin is distributed among the fiber, they not only crosslink themselves through the fiber networks, but also react with cellulose to form covalent bonding, thus preventing the breakage of fiber bonding by water.

Wet strength resins are required in different kinds of paper grades, such as: wallpaper, Kraft paper, filter paper and absorbent towel papers. The major wet strength sizes are: urea-formaldehyde, melamine-formaldehyde, used in acidic paper production, polyamide-epichlorohydrin (PAE) and polyvinylamine (PVAm).

PAE resin is a widely used wet strength resin in pulp and paper industry, which was first investigated in the 1950s.[21] The mechanism of PAE resin is shown in Figure 9. Its precursor is made by polycondensation reaction of polyalkylenepolyamine with a dibasic acid, and then reacts with epichlorohydrin to form the PAE resin.[21] The azetidinium groups have two possibilities for reaction. Espy et al. has shown that the azetidinium groups in PAE resins may form ester linkage with carboxyl groups on the cellulose fibers.[22] The other is to react through amine groups of other resin molecules to give a homo-crosslinked network.[23] Meanwhile, the cationic property of PAE resins ensures their absorbtion to negatively charged paper fibers, permanent bonds are formed upon heating at the dry section of the paper machine.[20]

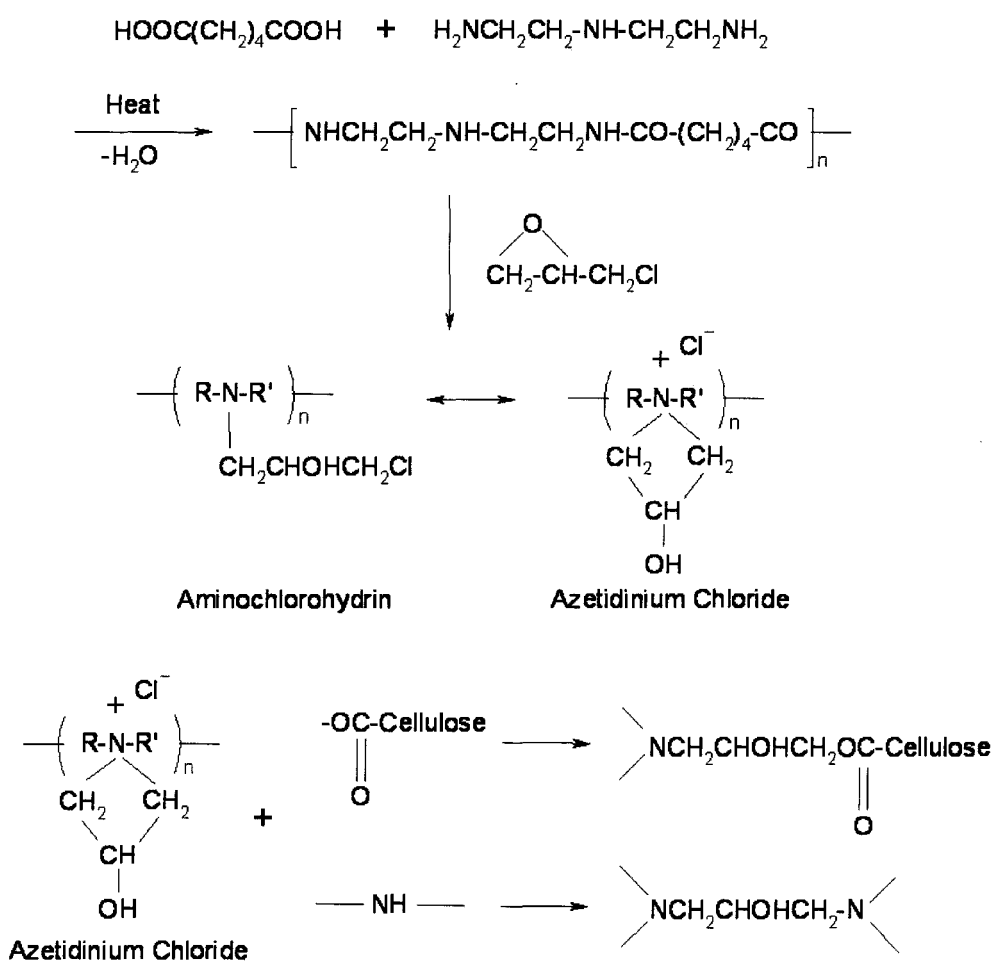

Figure 9: The mechanism of PAE resin development.

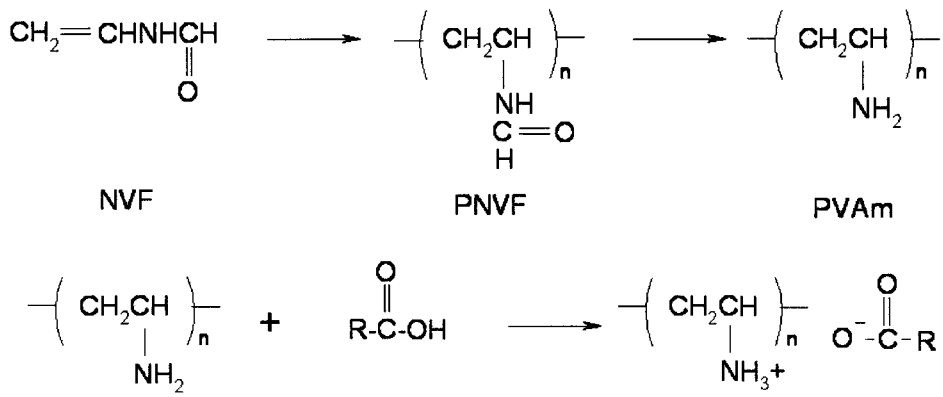

Figure 10: The mechanism of PVAm resin development

PVAm is a relatively new commercial polymer used in pulp and paper industry, which has a linear hydrocarbon chain with primary amine group on alternative carbons.[24] The increased interest in using PVAm as paper additive is because PVAm could be prepared from the hydrolysis of poly(N-vinylformamide) PNVF (Figure 10).[25] The amine groups in PVAm may react with carboxyl groups on the cellulose to form ammonium carboxylate in terms of application in the papermaking industry. Meanwhile, the cationic polymer can absorb to the negatively charged fibers through an ion-exchange process.[25] Geffroy et al. concluded the interaction between the cellulose and PVAm was purely electrostatic.[26]

2.4 Microgel

2.4.1 Microgel and polyNIPAM Microgel

Microgels are crosslinked polymers and colloid particles with average diameters ranging between 50 nm and 5 μm.[27] They can be easily characterized by the standard

colloid techniques like electrophoresis and dynamic light scattering. On the microscopic level, microgels are much like traditional hydrogels, and have been widely used in various industries, such as cosmetics, coating, food, oil recovery, drug delivery, and industrial processing.[28] Substantial work has investigated the gel response to different stimuli like ionic strength,[29] and electric response,[30] due to the interest in "Smart polymers." (Polymers can respond when stimuli like pH, temperature and ionic strength occur.)

Thermoresponsive microgels are the most important part of the stimuli-responsive microgels. The polyNIPAM based microgel has been researched extensively over the last several decades, and it was first investigated in our group[31]. The polyNIPAM microgel are thermo-sensitive because the linear polyNIPAM has a Lower Critical Solution Temperature (LCST) at about 32°C.[27] The monomer NIPAM is a major building block for temperature-sensitive microgels. It can undergo a fast free radical polymerization in aqueous solution to form polyNIPAM, and upon crosslinking, the linear polyNIPAM can be converted to the temperature-sensitive gel network to form the polyNIPAM microgel.[27] the microgel undertakes reversible volume phase transition between 32°C- 35°C (volume phase transition temperature, VPTT),[28] When the external temperature is above the VPTT, polyNIPAM microgel will exhibit sharp shrinkage, a unique property that makes the microgel an appropriate material for biomedical applications such as drug delivery, tissue engineering, and

enzyme immobilization.[32]

2.4.2 Functionalization of polyNIPAM microgel

There are two major limitations for applying the polyNIPAM-only microgels: the narrow range of the physical and chemical property and the lack of microgel reactive residue for further modification.[33] However, these limitations can be overcome by incorporating a functional group on the polyNIPAM Microgel. The advantages are: changing the volume phase transition behaviour of the microgel particle, providing the reactive-site for microgel post-modification, and different stimuli response properties for microgel.[33]

Among the functional groups, the carboxylic acid groups are most favourable, because they are pH-ionizable, and can provide the electrophilic sites for further chemical modification and bioconjugation. When ionized at high pH, carboxylic acid groups can increase the VPTT.[28] Karl et al.[34] and Dowding et al.[35] incorporated acrylic acid (AA) and methacrylic acid (MAA) into the polyNIPAM microgel particles *via* free radical copolymerization, and found that the functional group has a big influence on the volume phase transition behaviour of the microgels, the variation in pH could change the size of the functionalized microgel particle. However, both the AA and MAA readily form blocks with the polyNIPAM microgel, which would significantly weaken the post-modification of the functional groups.[36]

In our group, Hoare et al. prepared the vinylacetic acid (VAA) functionalized polyNIPAM microgel by copolymerization,[37] and his work showed the VAA-polyNIPAM microgels gives a sharp, highly thermal responsive profile. Upon ionization, this microgel displayed a much larger swelling response than the polyNIPAM by itself, and AA/MAA-polyNIPAM microgels. This indicates that the functional groups are highly localized on the surface of the microgel particles. The polyNIPAM-core/carboxylic shell microgel provides an ideal structure for applications like bioconjugation and medical diagnostics.

2.4.3 Bioapplication of the polyNIPAM microgel

Since the 1960s, the bio-application of hydrogels has been thoroughly studied, due to their potential biocompatibility.[38] From the 1980s, the research concerned with combining the gel and natural polymer such as collagen, has become very promising.[39] In current research, most of the work is focused on using gel for "tissue engineering" to regenerate the tissues and organs.

Initial work investigated the utilization of polyNIPAM-based sorbents in temperature-dependent chromatography. Different chromatography supports have been used, such as: porous glass, polymer particles and silica gel.[40] In addition, since the hydrophobic interactions were considered to determine the retention time of

protein in the polyNIPAM-based sorbents, some efforts tried to incorporate the hydrophobic site to polyNIPAM-based sorbents like polyNIPAM-coated particles,[41] polyNIPAM-grafted glass surfaces[42] The result proves that the surface hydrophobicity enhances the protein adsorption to the polyNIPAM-modified surfaces.

Other works used the thermosensitivity of the polyNIPAM microgels to adsorb and separate the proteins. Kawaguchi and co-workers performed the initial study of adsorption of proteins on polyNIPAM microgels.[43] The polyNIPAM microgel was prepared by precipitation polymerization and used the adsorbent of Human Gamma Globulin (HGG) at 25°C and 40°C based on the hydrophobic/hydrophilic property of polyNIPAM above/below the LCST. The amount of protein adsorption at 40°C was much higher than 25°C, which indicated that the higher temperature increased the hydrophobic character of the microgels, and more protein had been absorbed.

Hoffman[44] proposed a method of using ligand-grafted linear polyNIPAM to purify selected biomolecules. Another work by Silva and co-workers[45] explored the adsorption of human immunoglobulin IgG on polyNIPAM microgel. And amino group was incorporated in the microgel system as a functional group for further grafting of ligand with high specificity for human immunoglobulin.[46] Currently, polyNIPAM microgels have been extensively investigated in other areas such as: drug delivery,[47] medical diagnostics,[48] and sensor technology[49].

2.5 Streptavidin, biotin and streptavidin-biotin interaction.

The avidin-biotin system has been widely used as biotechnological research tool since the synthesis of biotin in 1941.[50] Its high affinity, high specificity makes it a general and useful system in many diverse applications.

2.5.1 Streptavidin (SP), avidin and biotin.

SP and avidin are similar proteins that are obtained from *Streptomyces avidinii* and egg white, with molecular weights of about 58 kDa and 67 kDa, respectively. The native units of SP have a molecular weight of 18 kDa. Both SP and avidin have four biotin binding sites per molecule. Avidin has an isoelectric point (pI) of 10, and the pI for SP is 5-6.5.[51] SP is extensively used to replace avidin because of its lower non-specific binding.[51] Biotin is a naturally existing vitamin in every living cell (Figure 11). The molecular weight of the biotin is 244.31,[52] and its molecular composition is $C_{10}H_{16}N_2O_3S$.

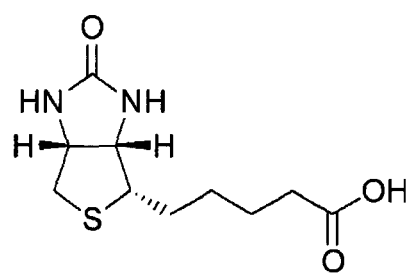

Figure 11: Biotin structure (from ref 51)

2.5.2 SP (avidin)-biotin interaction

The avidin-biotin interaction is the strongest noncovalent, biological interaction, as high as 10^{15} L·mol^{-1}, and SP has a similar affinity with biotin.[53] This high affinity ensures that binding is unaffected by different external conditions, like: pH, temperature, organic solvents and other agents. Second, the SP (avidin) –biotin interaction is highly specific, thus it would readily eliminate the unspecific binding. Meanwhile, both avidin and SP have four biotin binding sites, which can be modified without losing their binding ability with biotin.[54]

2.6 Coupling the SP to VAA-polyNIPAM microgels.

2.6.1 EDC

1-Ethyl-3-(3-dimethylaminopropyl)-carbodiimide (EDC) is the most popular carbodiimide in bioconjugation application, with a molecular weight of 191.7.[55] (Figure 12)

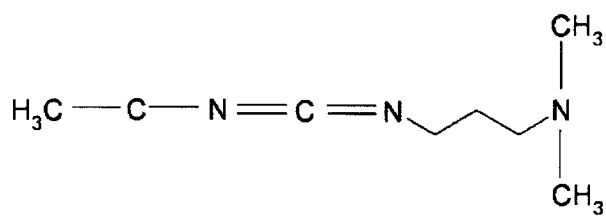

Figure 12: EDC structure

It can catalyze the amide formation between carboxyl groups and primary amine group.[55] The most common method for this conjugation occur when EDC first reacts with carboxylic acids to create an active intermediate (o-Acrylisourea), and then the

intermediate could react with the primary amine to form a stable amide bond, (Figure 13). However, the disadvantage is the intermediate is readily hydrolyzed and regenerates the carboxyl groups. This means that if the primary amine group does not find the target intermediate before it hydrolyzed, the conjugation would not occur.

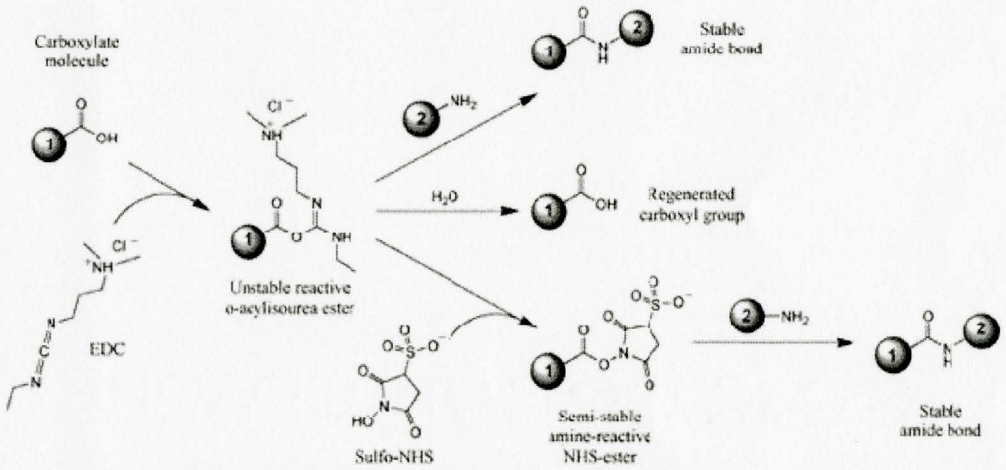

Figure 13: Different methods for EDC to react with carboxylate molecule (from Ref 57)

In another method, the EDC reacts with carboxylate groups and N-hydroxysulfosuccinimide (sulfo-NHS) to form a sulfo-NHS ester intermediate. Sulfo-NHS esters are hydrophilic active groups that readily react with amine groups.[56] The advantage of adding sulfo-NHS to the reaction is to increase the stability of the ester intermediate, which may increase the coupling efficiency.[57]

Staros et al. compared the EDC alone and EDC/sulfo-NHS methods to couple glycine to keyhole limpet hemocyanin, and the yield increased 20-fold using

sulfo-NHS rather than the EDC alone.[58] Debord et al. treated the polyNIPAM-AAc microgels with EDC-NHS, and the active ester intermediate displayed a remarkable stability that resisted degradation under standard hydrolysis protocols, however, when compared with EDC alone in terms of the coupling efficiency, the NHS step obviously decreased the overall yield of the coupling reaction.[59] Su in our group coupled the streptavidin with VAA-polyNIPAM microgels, which results in a surface coverage of 4×10^{-3} mg/m^2, however, it seems little undesirable flocculation occurred during the coupling reaction.[60]

2.6.2 Bradford protein assay

The Bradford protein assay is a simple method to measure the protein concentration in the solution. The principle involves the formation of a complex between Coomassie Brilliant Blue G-250 and proteins (Figure 14).[61] The dye has three forms: acidic (red), neutral (green) and basic (blue). In the acidic condition, the dye displays a red colour. When combined with protein, it is converted to a stable unprotonated blue form, causing an absorption maximum shift from 470 nm to 595 nm.[62,63] Then the dye-protein complex is detected at 595 nm using the spectrophotometer, and the amount of absorbance corresponds to the protein presents.

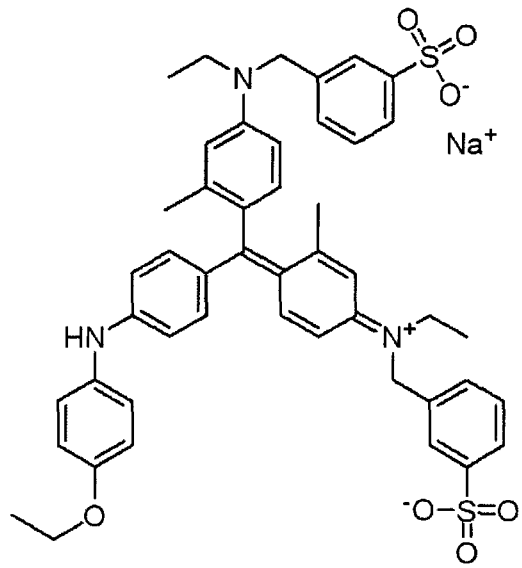

Figure 14: The structure of Coomassie (from Sigma-Aldrich)

2.7 Disk diffusion method

In the disk diffusion method, the filter paper impregnated with antimicrobial materials is placed on agar plates with bacterial lawn. After incubation, the antimicrobial susceptibility was determined by a clear inhibited zone around paper. The disk diffusion method for Antimicrobial Susceptibility Testing (AST) was developed in the 1940s.[64] Heatley used adsorbent paper to carry the penicillin antimicrobial solution.[65] Baucer et al. [66]and Rolinson et al. [67] tried to facilitate and standardize the disc susceptibility method by introducing the antimicrobial agents in known concentration. Then the modified method has been accepted as the disk diffusion standard by the standard national committee for clinical laboratory standards.[68] Tolba et al. immobilized cellulose binding modules (CBM)-phage onto filter paper, and used the disk diffusion method to measure the phage infectivity.[69]

Chapter 3: Experimental Section

3.1 Introduction

This chapter first described the phage and *E. coli* bacteria preparation and characterization. In addition, the method to investigate the influence of wet strength resin and its modified paper to phage activity was also described. Then the methods of polyNIPAM microgel preparation, streptavidin coupling and phage immobilization were presented.

3.2 Materials

N-Isopropylacrylamide (NIPAM, 97%, Sigma-Aldrich) was recrystallized with toluene and hexane mixture (ratio: 60/40) before using, N,N-Methylenebisacrylamide (MBA, 99%, Aldrich), Vinylacetic acid (VAA, 97%, Aldrich), Ammonium persulfate (APS, 99%, Fisher Scientific) were all used as received. Milli-Q water was used in the polymerization. Streptavidin (SP, Sigma), N-ethyl-N'-(3-dimethylaminopropyl) carbodiimide hydrochloride (EDC, Sigma), 2-(N-morpholino) ethanesulfonic acid (MES, sigma), Sodium phosphate monobasic (NaH_2PO_4, Sigma), Sodium phosphate dibasic (Na_2HPO_4, Sigma), Bradford reagent (Sigma), Bovine serum albumin standard solution (BSA, Sigma), Hydroxy-2,5-dioxopyrrolidine-3-sulfonicacid sodium salt (Sulfo-NHS, Sigma), Polyvinylamine (PVAm, 0.5%) is provided by Wei Chen, Tryptone and Agar, granulated are purchased from Becton, Dickinson and Company,

TWEEN 20 detergent (Merck KGaA, Germany), *E. coli* bacteria, T4 phage with genetically biotinylated capsid heads and wild phage are provided by Tolba, M and Dr. Griffiths, M (University of Guelph, Canada), Polyamide-epichlorohydrin (PAE, 20wt%, Hercules, USA).

3.3 Phage and *E. coli* bacteria preparation

3.3.1 Preparation of LB media, top agar and agar plates.

LB media: 10g tryptone, 10g sodium chloride (NaCl) and 5g yeast extract were added to 900 ml water, adjusted to pH 7.5 with NaOH, the volume was adjusted to 1L with water, and then sterilized in autoclave. (50ml in 250ml conical flask)

Top agar: 10g tryptone, 8g NaCl and 5g agar were dissolved in 1L water with stirring and heating, and divided into tubes of 5 ml, covered at the top with cotton and aluminium foil, then sterilized in autoclave.

Agar plates: 10g tryptone, 8g NaCl, 5g agar and 1L water were mixed in a 2L flask, and sterilized in autoclave. After sterilization, the flask was gently stirred to evenly distribute the media, then poured 20ml of LB agar media in each Petri dish (size: 100×15mm), which was inverted in the fume hood overnight. Then the plates were stored in the 4°C refrigerator for future use.

3.3.2 Preparation of *E. coli* bacterial solution.

A single colony of *E. coli* bacteria was taken from a plate using a sterilized loop and added to 1 ml of LB media (1L water, 10g tryptone, 10g sodium chloride, 5g yeast

extract), prior to overnight incubation at 37°C with moderate agitation.

3.3.3 Preparation of phage stock solution.

100 μl of *E. coli* stock solutions were mixed with 5 ml molten top agar, and gently shook for few seconds, then the entire media was poured onto agar plates, presence of air bubble was avoided and plates were swirled gently to ensure even distribution. After solidification, 100 μl of phage solution was dropped (at least 10^6 pfu/ml) in the middle of the plate, and the plates were incubated overnight at 37°C. After removing the plates from the incubator, 5 ml of lambda buffer (1L water, 5.8g NaCl, 2g $MgSO_4$, 50ml 1M Tris buffer pH 7.5, 0.1g gelatine) were added to the plate, and the top agar was scraped off with a sterilized loop, then transferred to a large centrifuge tube, and 5 ml of chloroform was added to the suspension, allowed by 15 minutes incubation. The tube was centrifuged for 10 minutes (6000 rpm, 25°C), and the aqueous layer was filtered through a 0.2 μm syringe filter. The collected solution contained the phages.

3.3.4 Infection of plating bacteria.

The phage solution was serially diluted by mixing 100 μl of phage solution with 900 μl of lambda buffer; then 100 μl phage solution and 100 μl of *E. coli* bacterial solution were added to the 5 ml top agar tube. The tube was gently shaken and incubated at Room Temperature (RT) for several minutes to ensure that the phage attached to the *E. coli* bacteria. The entire contents of the tubes were poured onto LB plates, and air bubble was avoided with gently swirling the plate to ensure even

distribution, then the plates were incubated overnight at 37°C with moderate agitation. The plates were removed from the incubator, and the individual plaques were counted and the concentration of phage solution (pfu/ml) was calculated.

3.4 Treatment of the paper sample with wet strength resin

PAE resin: Whatman #1 filter paper (diameter: 6 mm) were soaked in different PAE resin solutions (0.1%, 1%, 2%, 10%wt) for 30 minutes. The dry and wet paper samples were weighed, and the paper samples were placed on the speed dryer at 120°C, for 10 minutes to ensure that the PAE resin crosslinked with paper fibers. The PAE content on paper was determined by the weight difference of dry and wet sample multiplied by the concentration of the resin solution.

PVAm resin: 20 μl PVAm resin solutions (0.1%, 0.5%) were dropped onto the Whatman #1 filter paper surface (diameter: 6 mm) for 30 minutes, the dry and wet paper samples were weighed, the method for determining the PVAm content on the paper was the same as PAE resin.

3.5 Coat the phage to treated paper and detect the *E. coli* bacteria.

Different paper samples (filter paper, PAE/PVAm treated paper) were soaked in 2 ml phage solution and MG-Phage solution overnight. The samples were removed from the solution, washed in 2 ml lambda buffer twice, and dried in the fume hood for 30

minutes. Then 100μl *E. coli* bacterial solution was added to 5 ml molten top agar, gently shook, then the entire contents were poured onto LB plates, waiting several minutes for solidification, and the phage coated paper samples were attached onto the top agar layer. Wetting the paper surface with little lambda buffer allowed the phages to move easily. Then the plates were incubated overnight at 37°C with moderate agitation. The infection of phage was determined by a clear inhibited zone (lysis) around the paper surface.

3.6 Microgel preparation and characterization.

The PolyNIPAM microgel functionalized with carboxyl group at the outer layer was prepared as described in literature.[37] Polymerization was conducted in a 500 ml three-necked flask with a condenser and a glass stirring rod. 12.4 mmol NIPAM, 0.65 mmol MBA, 0.17 mmol SDS and 1.2 mmol VAA were dissolved in 150 ml of water, heated to 70°C, and deoxygenated by bubbling with nitrogen for 30 minutes. Then 0.44 mmol APS was dissolved in 10 ml of water and poured into the flask to initiate the polymerization. The reaction was conducted overnight under 200 rpm mixing. After polymerization and cooling, the microgel solution was purified several times by ultracentrifugation (Beckman model Optima L-80 XP 50 minutes at 50,000 rpm), until the conductivity of supernatant was less than 5 μs/cm. Then the microgels were lyophilized and stored at 4°C refrigerator for future using.

3.7 Coupling streptavidin (SP) to microgel (MG)

Two different methods were carried out: coupling with EDC, and EDC-NHS.

3.7.1 Coupling with EDC (MG-SP-EDC)

The coupling method was followed the description in literature.[60] Lyophilized microgel was dissolved in MES buffer (20mM, pH 5.5) at a concentration of 2 mg/ml overnight. 1 ml microgel suspension was reacted with 77 μl SP (0.63 mg/ml) under 100 mM EDC for 4 hrs at RT. After reaction, microgel was purified by ultracentrifugation (50 minutes, 50,000 rpm), and washed twice by 2 ml MES buffer with stirring for 30 minutes, then resuspended in 1 ml MES buffer. A control in which microgel reacted with streptavidin was done without EDC. The amount of SP coupled on the microgel surface was measured by a UV-VIS spectrophotometer (Beckman Coulter, DU 800) with the Bradford micro assay.

3.7.2 Coupling with EDC-NHS in MES buffer (MG-SP-NHS-1) and sodium phosphate buffer (MG-SP-NHS-2).

Lyophilized microgel was dispersed to a concentration of 2 mg/ml in MES buffer (20mM, pH 5.5). Then 5 mM EDC and 7 mM sulfo-NHS were added to 1ml microgel suspension, and incubated for 15 minutes at RT, and 77 μl SP (0.63 mg/ml) was added to the solution. For "MG-SP-NHS-2", 0.4 ml sodium phosphate buffer (0.1M, pH 7.4) was added to the solution to bring pH of the coupling medium above 7. Reaction was carried out at least 2 hrs at RT with stirring. The excess reactants were removed by washing and ultracentrifugation twice (50 minutes, 50,000 rpm) in 2 ml sodium

phosphate buffer, then the microgel solution was resuspended in 1ml sodium phosphate buffer. A control (MG-SP) was done without EDC-NHS. The amount of coupling SP was measured by the Bradford micro assay.

3.7.3 Procedure for Bradford micro assay.

- Prepared BSA standard protein solution in MES buffer (20mM, pH 5.5) and sodium phosphate buffer (0.1M, pH 7.4) ranging from 1-10 μg/ml.
- Added 1 ml buffer (blank sample), 1 ml different BSA standard solution and 1ml Bradford reagent to cuvettes, and incubated for 10 minutes.
- Prepared 1ml unknown samples with an approximate concentration between 1-10 μg/ml, then mixed with 1ml Bradford reagent, incubated for 10 minutes.
- Measured the absorbance at 595 nm using spectrophotometer.
- Plotted the net absorbance vs. BSA concentration of each sample as the standard curve.
- Determined the concentration of unknown samples by comparing with the standard curve.

3.8 Immobilize phage to streptavidin coupled microgel (MG-Phage)

500μl MG-EDC was reacted with 500μl phage solution (at least 10^8 pfu/ml) for at least 2 hrs. After the reaction, the microgel was centrifuged and washed with 2 ml TWEEN 20 detergent, and 2 ml Lambda buffer, then resuspended in 500μl Lambda buffer with stirring for 30 minutes. Then the same procedure was followed as

"infection of plating bacteria" to measure the concentration of remaining phage on the microgel particles.

3.9 Particle sizing

Particle size of the microgel was determined by dynamic light scattering (Brookhaven Instruments Corp). The laser was conducted at 633 nm as the light source. Samples were prepared by dissolving in filtered 1 mM KCl, and the scattering intensity was kept between 100 to 250 kilocounts/s. Sample pH were adjusted by 0.1 M KCl and 0.1 M NaOH. At least three replicates were conducted for each sample, the error bar indicates the standard deviation of the measurement.

3.10 Electrophoretic mobility

Electrophoretic mobility was measured using the Zeta Potential Analyzer (Brookhaven Instruments Corp), and operated in Phase Analysis Light Scattering (PALS). Sample preparation and pH adjusting were the same as described in particle sizing measurement. A total of 10 run (each consists of 20 cycles) were conducted for each sample.

Chapter 4: Results and Discussion:

4.1 Bacteriophage and *E. coli* bacteria preparation.

Enumeration of the *E. coli* bacteria was performed by plate count technique and expressed in cfu/ml. and enumeration of phage was carried out by agar overlay technique and expressed in pfu/ml. The overnight incubation of *E. coli* bacterial solution could reach a concentration of 10^6 cfu/ml.

After infection of plating bacteria and overnight incubation, the phage solutions had a concentration of 10^9 pfu/ml. Figure 15 shows the biotin-phage solutions with different concentrations of infected *E. coli* bacteria in the plates. In the control sample without phage solution, infection did not appear. In the 10^{-1} plates (high concentration), almost all the yellow background had disappeared, which indicated that nearly all the bacteria in the plates were infected due to the high concentration of biotin-phage solution; As the concentration of biotin-phage solution decreased, less bacteria were infected as shown in the plates. Until the 10^{-7} plates, 73 infection phage plaques were found on the plates.

The concentration of the phage solution (pfu/ml) = number of plaques on plate × 10^n (n: diluted times) × 10. Thus, the concentration of the phage solution in Figure 15 was: 7.3×10^9 pfu/ml. For each sample, two plates were measured, and the mean

concentration was calculated.

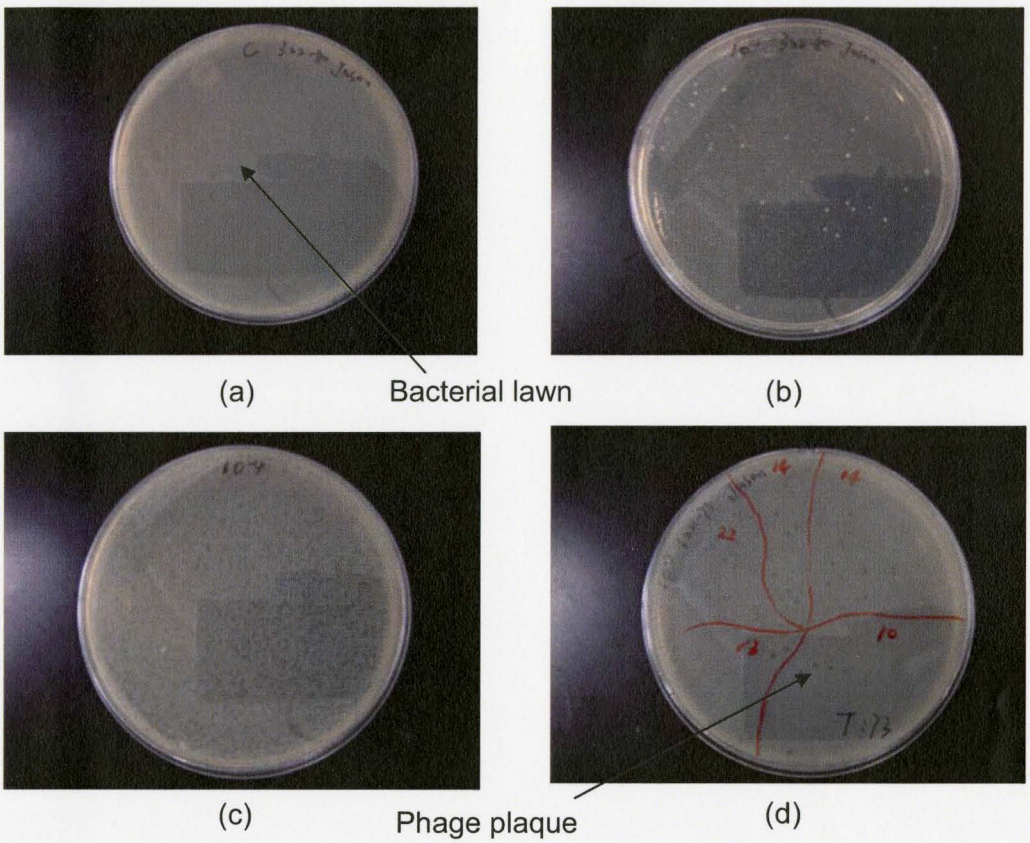

Figure 15: Different concentrations of biotin-phage solutions infected *E. coli* bacteria in the plates. (a) Control sample without biotin-phage solution. (b) 10^{-1} of the original biotin-phage concentration. (c) 10^{-4} of the original biotin-phage concentration. (d) 10^{-7} of the original biotin-phage concentration.

4.2 Mobility and size of biotin-phage and T4 wild phage particle.

The Measurement of mobility and size of biotin-phage and T4 wild phage were performed in lambda buffer (0.1M NaCl and 0.017M $MgSO_4$), and results were presented in Table 1. Electrophoretic mobility, defined as velocity of charged particle divided by the electric field strength, characterises part of particle's surface charge.

The result in Table 1 shows that both biotin-phage and T4 wild phage have the same mobility value of -1.23×10^{-8} m^2/Vs, which means both samples carry the negative charge at pH 7.5. The anti-coli bacteriophage was first reported to bear a negative charge from pH 3.4 to pH 9.0 by Krueger et al.,[70] and its isoelectric point is around 2.9.[71] Childs et al. stated that the proteins located at the surfaces of T4 phage particles, such as major head protein, soc and hoc protein (isoelectric point of 4.1[72]), could largely effect the negative charge of T4 phage particle.[73]

Light scattering data in Table 1 shows the size of biotin-phage and T4 wild phage, which are 117 ± 1.5 and 115 ± 2 nm respectively. Dynamic light scattering is a technique based on the measurement of intensity fluctuations of light scattered by particles, the fluctuation is caused by particle moved in Brownian motion. So the diameter results were related to the particle diffusion coefficient and no phage shape effect was considered, the result below indicated the phage particles were not aggregated. Dabrowska et al. did a similar measurement and reported T4 phage with a size of 131 ± 0.5 nm.[74]

Table 1: Mobility and size of T4 biotin-phage and T4 wild phage at pH 7.5

	Electrophoretic mobility ($\times10^{-8}$ m^2/Vs)	Hydrodynamic diameter (nm)
Biotin-phage	-1.23 ± 0.09	117 ± 1.5
T4 wild phage	-1.23 ± 0.17	115 ± 2

4.3 Coat unsupported biotin-phage to paper surfaces.

4.3.1 Treatment of paper surfaces with wet strength resins. (PAE and PVAm)

The Whatman #1 filter paper was treated with different concentration of PAE as shown in Table 2. The percentage of PAE on paper increased linearly with the PAE concentration. As to the PVAm treatment, 20 μl of PVAm solution (0.1%, 0.5%) was dropped on Whatman #1 filter paper, which equals 20 μg, 100 μg PVAm on the paper surface respectively.

Table 2: The amount of PAE resins treated on filter paper

Concentration of PAE	Dry weight (mg)	Wet weight (mg)	Mass of PAE on paper (mg)	% PAE/dry paper
0.1%	3.4	13.8	0.0104	0.3
1%	3.4	15.4	0.12	3.5
2%	3.4	15.4	0.24	7
10%	3.4	15.7	1.23	36.2

4.3.2 Coat unsupported phage to filter paper and detect *E. coli* bacteria.

As described before, the coating process involves soaking filter paper in phage solution overnight and washing the paper twice with buffer. Table 3 indicates the number of phage captured by filter paper measured by pour plate technique, and only 7.1% of the unsupported T4 phages could be captured by filter paper due to physical adsorption. In Figure 16, a clear inhibited area (lysis) appeared on the plates without washing the filter paper, which indicates that the phages on filter paper could infect *E.coli* bacteria. However, the lysis disappeared and most of the phages lost their

infection after washing the paper twice with lambda buffer, this implies that filter paper has low phage adsorption and weak adhesion to phage particle because of the electrostatic repulsion, and direct coating of unsupported phage to filter paper was not a promising way for bioactive paper application. Tolba et al. solved this problem by immobilized cellulose binding modules (CBM)-phage onto filter paper, and successfully detected *E. coli* bacteria even after washing.[69]

Table 3: The number of unsupported T4 phages captured by filter paper (Whatman #1)

	Original pfu	pfu after soaking	pfu of first washing	pfu of second washing	Total phage captured by paper	% phage captured by paper
Filter paper	1.12×10^{8}	1×10^{8}	2.6×10^{6}	1.4×10^{6}	8×10^{6}	7.14

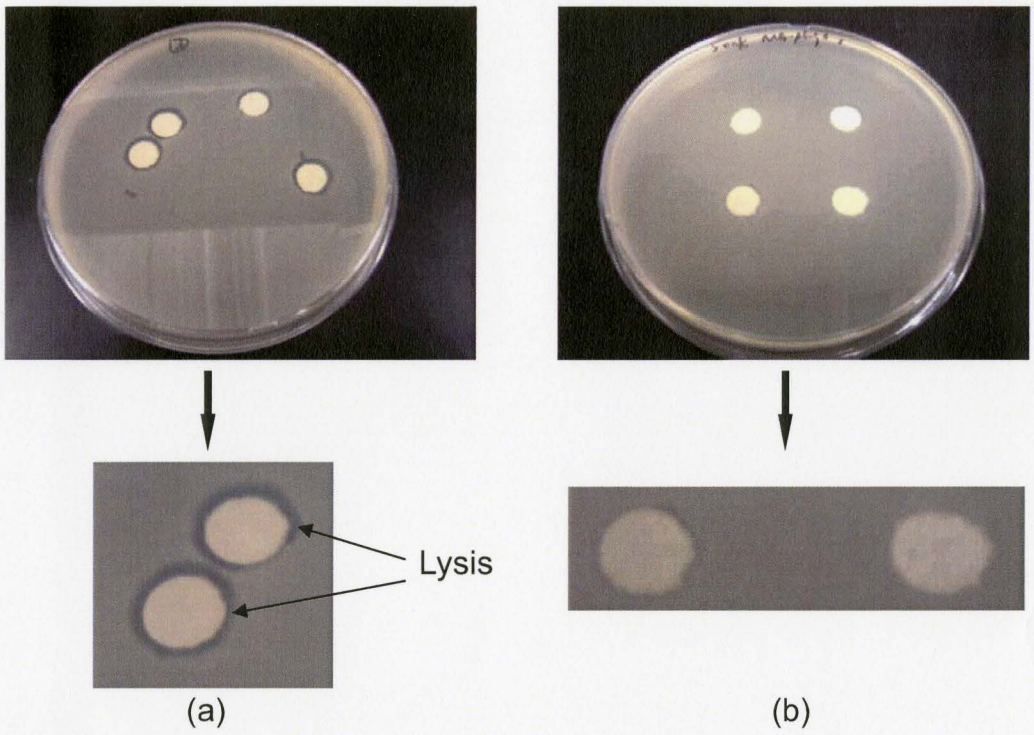

Figure 16: Lysis of unsupported phage on filter paper (Whatman 1).
(a) Unsupported phage on filter paper before washing. (b) Unsupported phage on the filter paper after washing.

4.3.3 Coat unsupported phage to PAE treated paper.

Filter paper was treated with different concentration of PAE resins as described. Table 4 shows the number of unsupported phage captured by different PAE treated paper without heating. In Table 5, all the PAE treated paper were heated on the speed dryer for 30 minutes in order to form the permanent bonds between polymer and fibers.

Table 4: The number of unsupported phage captured by PAE paper (no heat curing)

	pfu of original	Total pfu captured by paper	**% pfu captured by paper**
Filter paper	1.12×10^8	8×10^6	**7.14**
0.1% PAE	1.23×10^8	1.13×10^8	**91.9**
1%PAE	1.23×10^8	1.2×10^8	**97.6**
2%PAE	1.23×10^8	1.22×10^8	**99.2**
10%PAE	1.23×10^8	1.23×10^8	**>>99**

Table 5: The number of unsupported phage captured by PAE paper (after heat curing)

	pfu of original	Total pfu captured by paper	**% pfu captured by paper**
Filter paper	1.12×10^8	8×10^6	**7.14**
0.05% PAE	1.23×10^8	4.3×10^7	**35.0**
0.1%PAE	1.23×10^8	4.2×10^8	**34.1**
1%PAE	1.23×10^8	4.8×10^8	**39.0**
2%PAE	1.23×10^8	5.3×10^8	**43.1**

The results in Table 4 indicate that a little amount of PAE on paper could generate a significant difference to the phage capture percentage (from 7.14% to 91.9%). This is because the anionic property of phage particle enables them to readily absorb to the positively charged PAE resins on the paper through electrostatic interaction.

Table 5 shows that the number of captured phage decreased a lot after the PAE treated paper was been heated. For example, as to the 0.1% PAE paper, the percentage of captured phage decreased from 97.6% to 34%. Upon heat curing, most PAE resins migrate beneath the surface of cellulose fibers and form the network of water-insoluble bonds between the fibers, which could explain the decrease of

captured phage.

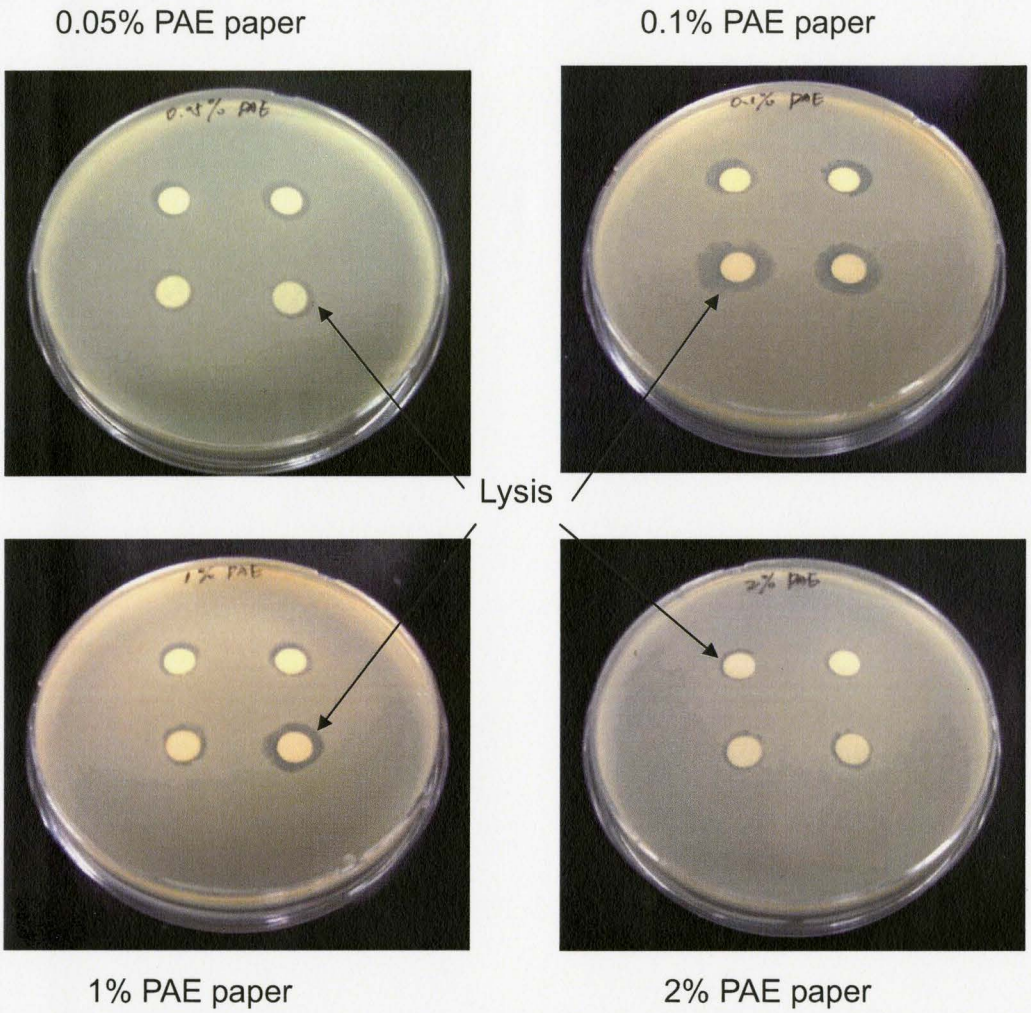

Figure 17: Phage infection from PAE treated paper before washing

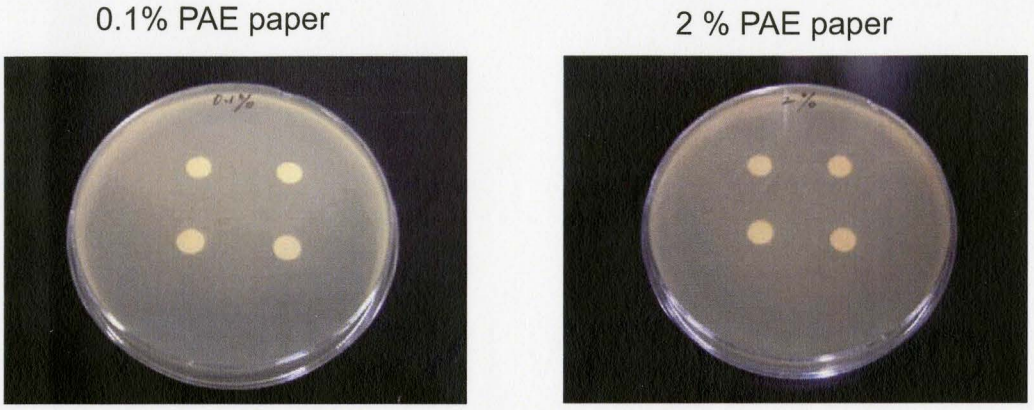

Figure 18: Phage infection from PAE treated paper after washing.

Figure 17 shows the phage infection from different PAE papers before washing. Clear lysis on the plates after overnight incubation indicates that some phage on PAE paper could detect bacteria before washing, and directly coating phage solution to PAE paper did not completely deactivate the phage infection. However, the results in Figure 18 show that the lysis disappeared and unbound phages were removed from PAE paper by washing. The reason was because heating process weakened the adhesion between phage and PAE treated paper as shown in Table 4 and Table 5. Compared with filter paper, PAE treated paper has higher phage binding efficiency because of the electrostatic interaction, but low phage activity was exhibited, most of the phage captured by PAE paper couldn't detect bacteria anymore.

4.3.4 Coat unsupported phage to PVAm treated paper.

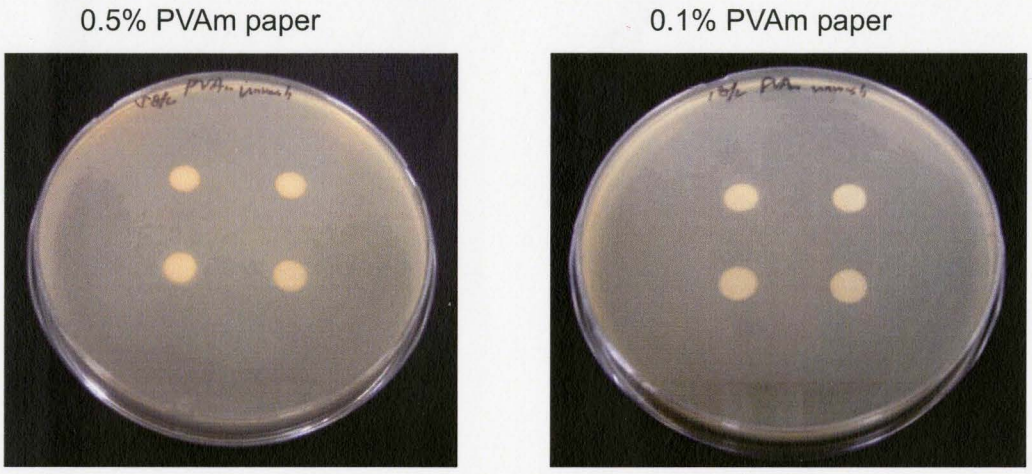

Figure 19: Phage infection from PVAm treated paper before washing

Figure 19 revealed the phage infection from PVAm treated paper before washing. No lysis was found on both of the plates, which indicated that the unsupported phages were deactivated after being directly coated on PVAm treated paper before washing.

To confirm the PVAm solution would deactivate phage infection, another experiment was performed where 100 µl unsupported biotin-phage solution (original concentration is 2.45×10^{8} pfu/ml) was mixed with 100 µl 0.1% PVAm solution for 2 hrs with stirring. The result in Table 6 shows that almost all the phages have been deactivated after mixing, which implies that PVAm had strong phage adsorption and almost completely deactivated the phage particle because of the electrostatic interaction. Geffroy et al. investigated the adsorption of PVAm onto cellulose and they

concluded that the interaction between the cellulose and PVAm was purely electrostatic.[26] The adsorption of human viruses (negative charged particles) to different polymers including PVAm was examined by Sirotkin et al., positive charged PVAm and polyallylamine (PAAM) exhibited a strong affinity for viral particles than negative charged polymer poly(methacrylic acid) (PMAA) and they concluded the electrostatic interaction played an important role in the adsorption of viral particles to synthetic polymers.[75]

Table 6: The number of active phage in original and PVAm solution

	Active phage number (pfu)
Original	2.45×10^{7}
0.1% PVAm-phage	0

The results in PAE/PVAm paper proved that direct coating of unsupported phage to wet strength resin treated paper was not a promising method for bioactive paper application.

4.4 Synthesis and characterization of the VAA-PolyNIPAM microgel

The VAA-PolyNIPAM microgel was prepared by polymerization among NIPAM monomer (0.87 wt %), VAA functional monomer (0.066 wt %), MBA (0.062 wt %), SDS (0.03 wt %) and APS (0.062 wt %). The carboxyl acid group contents in microgels were 0.25 ± 0.02 mmol/g measured by potentiometric and conductometric titrations as described before.[37] Previous work showed that the functional groups

(carboxyl acid groups) were located at the surface of the microgel particle,[37] which facilitates bioconjugation applications.

Figure 20 shows temperature dependence of the hydrodynamic diameter of VAA-microgel particle at pH 3.5 and pH 10. As pH increased from 3.5 to 10, the microgel particle was transferred from protonated state to fully ionized state and its diameter increased significantly due to the ionization of carboxyl acid groups.[37] This indicates that most of the carboxylic acid groups were localized at the surface of the microgel particle. Meanwhile, the Volume Phase Transition Temperature (VPTT) was observed in the microgel particle at pH 3.5 between 25°C-40°C for the pure polyNIPAM microgel[27]. This implies that functionalized VAA doesn't change the thermosensitivity of the polyNIPAM microgel.

The pH dependence of electrophoretic mobility of the VAA-microgel particle at 25°C is shown in Figure 21. The negative charge of the microgel increased dramatically as the pH increased, especially in the narrow range of pH 4-6, due to the ionization of carboxyl acid groups at the surface of the microgel particles,[37] which provides ideal reactive sites for microgel postmodification.

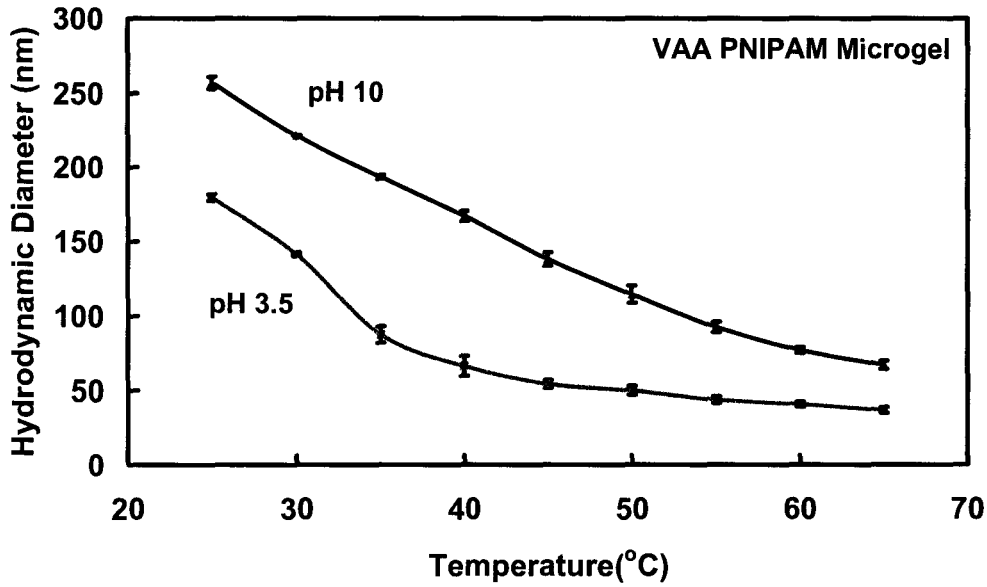

Figure 20: Temperature dependence of the hydrodynamic diameter of the VAA-PNIPAM microgel at pH 3.5 and pH 10.

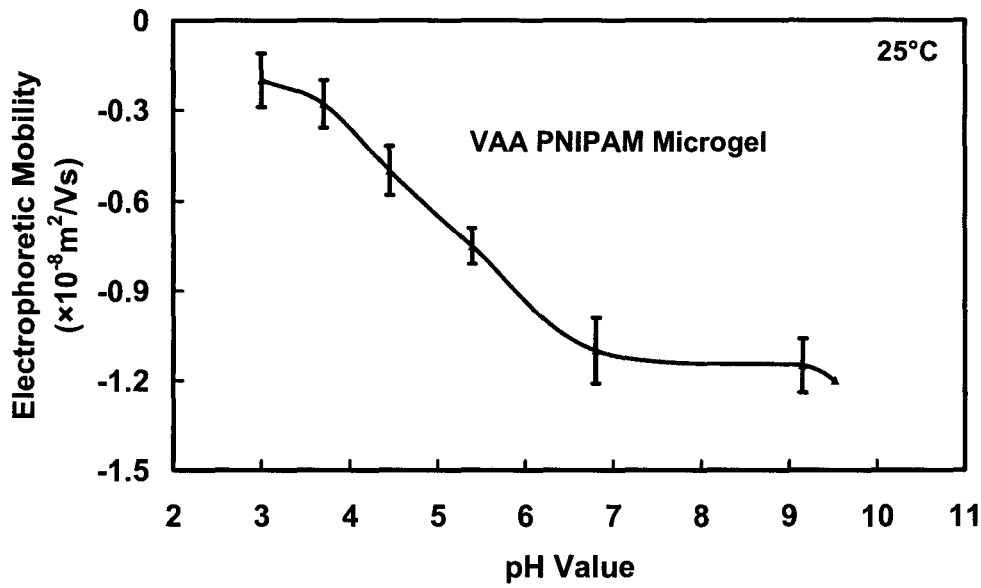

Figure 21: pH dependence of mobility of VAA-PNIPAM microgel at 25°C.

4.5 Coupling streptavidin to microgel.

Three different methods were used for the coupling experiments ("SP-MG-EDC", "SP-MG-NHS-1", "SP-MG-NHS-2"), then Bradford micro assay was used to measure the concentration of SP on the microgel particle. Figure 22 illustrates the methodology of coupling SP to microgel and immobilizing biotin-phage to MG-SP.

4.5.1 Calibration curve

Before the experiment, BSA standard protein solutions were used to generate calibration curves for both MES buffer and sodium phosphate buffer. See Appendix 1.

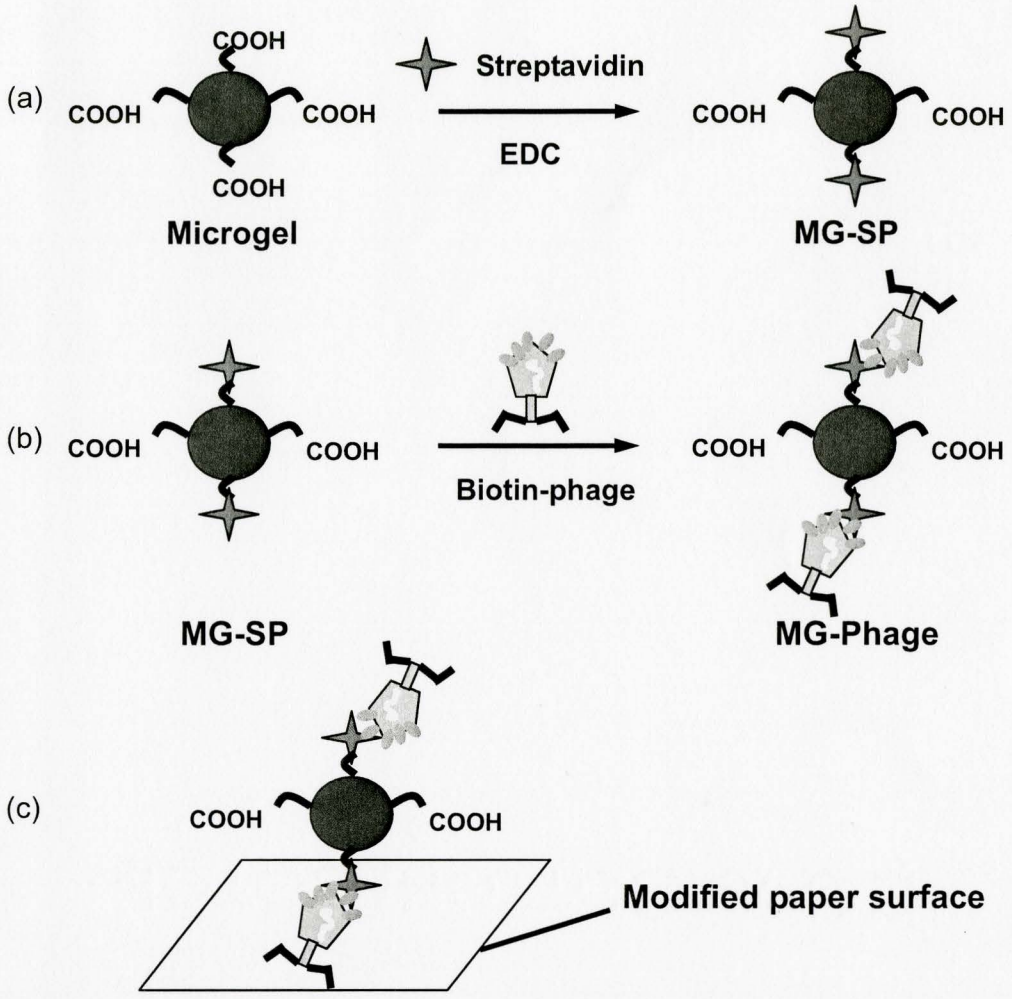

Figure 22: (a) Couple SP onto microgel particle. (b) Immobilize biotinylated phage to MG-SP. (c) Coat microgel supported phage to modified paper surface and detect *E. coli* bacteria.

4.5.2 The amount of coupled SP on microgel particle

The original amount of SP was: 77 μl × 0.63 mg/ml = 48.5 μg. The amount of SP coupled to microgels in three different methods (MG-SP-EDC, MG-SP-NHS-1, MG-SP-NHS-2) is shown in Figure 23: (Blue columns refer to the amount of coupled SP in different methods; Purple columns refer to control samples, in which the reactions were performed without EDC and EDC/NHS; The light yellow columns

refer to another series control samples, in which only microgel was measured in MES and sodium phosphate buffer. The errors represent the standard deviation of the mean concentration.)

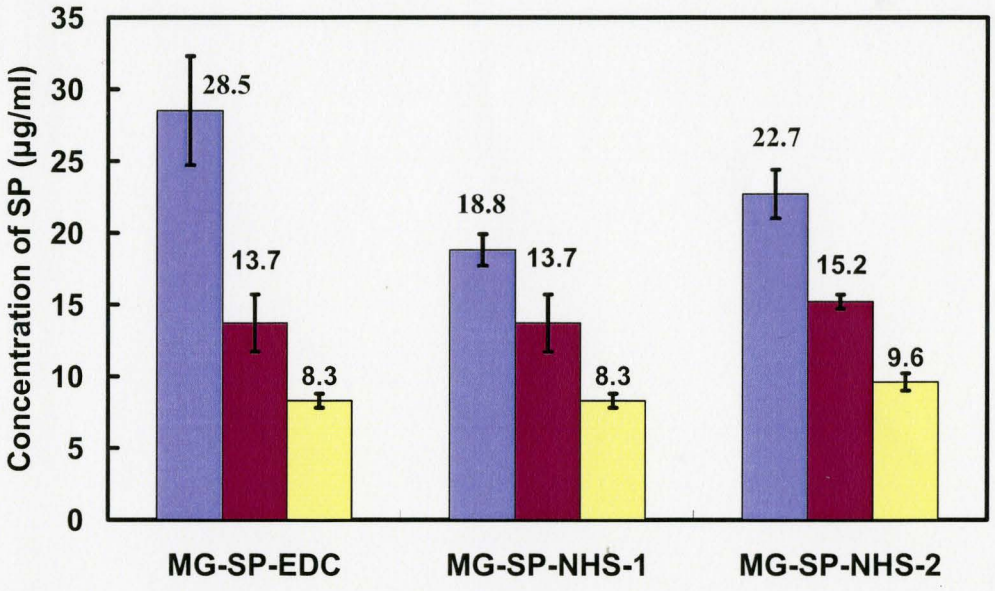

Figure 23: The amount of SP coupled on microgels

In the first method of coupling only with EDC in MES buffer (MG-SP-EDC), the measured SP concentration increased from 8.3 μg/ml to 28.5 μg/ml. This confirms that SP has been coupled to microgel particles. In the presence of EDC, the SP concentration increased from 13.7 μg/ml to 28.5 μg/ml, corresponding to an increase of coupling efficiency from 11.3% to 42.1%, which proves EDC catalyzed the SP coupling reaction. There are 20.2 μg SP coupled to microgel, which corresponds to a coverage of 0.23 mg/m^2 (See Appendix 2 for calculating surface coverage of SP on

microgel). A similar approach has been investigated by Huang et al. with coupling SP to polystyrene (PS) latex, and resulted with a SP surface coverage of 4.8 mg/m^2.[76]

As to the method of coupling SP with EDC/NHS, SP could still couple to the microgel as the measured SP concentration increased to 18.8 μg/ml (MG-SP-NHS-1) and 22.7 μg/ml (MG-SP-NHS-2). However, the NHS step decreased the overall yield of the coupling reaction, compared with MG-SP-EDC (from 28.5 μg/ml for MG-SP-EDC to 18.8 μg/ml for MG-SP-NHS-1 and 22.7 μg/ml for MG-SP-NHS-2). The advantage of adding sulfo-NHS is to increase the stability of the intermediate, which could be readily hydrolyzed in MG-SP-EDC, however, the amine-reactive NHS ester is too stable to form amide bond with amine groups, thus decreasing the overall coupling efficiency. Debord et al. investigated the unusual stability of succinimidyl esters in polyNIPAM-AAc microgels, and observed a similar result when coupled EDC and EDC/NHS to polyNIPAM-AAc (Acrylic Acid) microgel.[59] MG-SP-EDC had the highest SP concentration among the three methods, and it was used for further reaction with biotin-phage solutions.

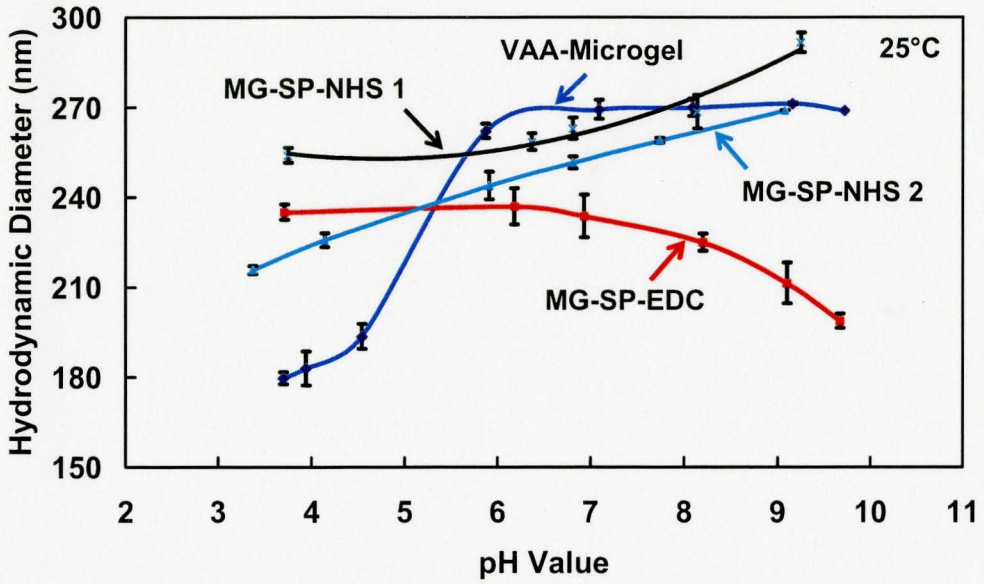

Figure 24: pH dependence of the hydrodynamic diameter of MG-SP-NHS 1, MG-SP-NHS 2 and MG-SP-EDC compared with VAA-Microgel.

The light scattering data in Figure 24 shows the pH dependence of hydrodynamic diameters of different microgels. The diameter of VAA-Microgel increased with pH due to ionization of the carboxylic acid groups. After the coupling reaction, the treated microgel shows a larger diameter than VAA-Microgel at low pH, which increased from 180 nm to 235 nm in MG-SP-EDC, indicating that the coupling reaction generated a little aggregation. Su et al. obtained a double sized MG-SP using the same method.[60] When comparing the two results of microgel coupling with EDC/NHS, the diameter of MG-SP-NHS 1 is slightly higher than MG-SP-NHS 2, because the coupling of MG-SP-NHS 1 occurred at pH 5.5 (MES buffer), which is lower than the isoelectric point (pI) of SP, and SP should carry a slightly positive charge, which facilitates a little aggregation with negative charged VAA-microgel.[60]

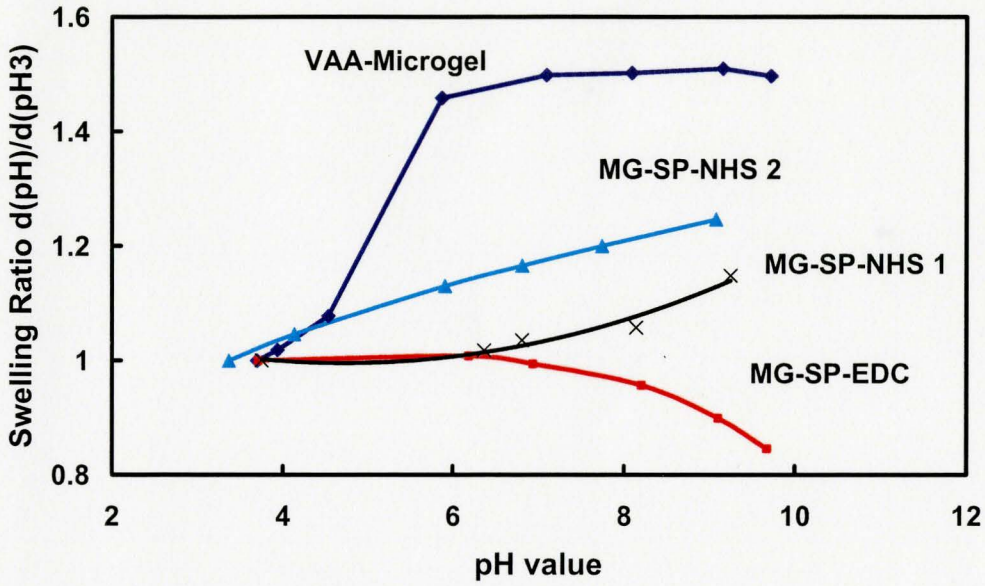

Figure 25: pH dependence of the swelling ratio of VAA-Microgel, MG-SP-NHS1, MG-SP-NHS2 and MG-SP-EDC.

The swelling ratios in Figure 25 were calculated by dividing the measured particle size at different pH by the same microgel at lowest pH (pH =3). After coupling with SP in the presence of EDC and EDC/NHS, the narrow range of ionization for VAA-Microgel disappeared, which confirms the carboxyl group located at the surface of VAA-Microgel reacted with EDC, EDC/NHS and SP.

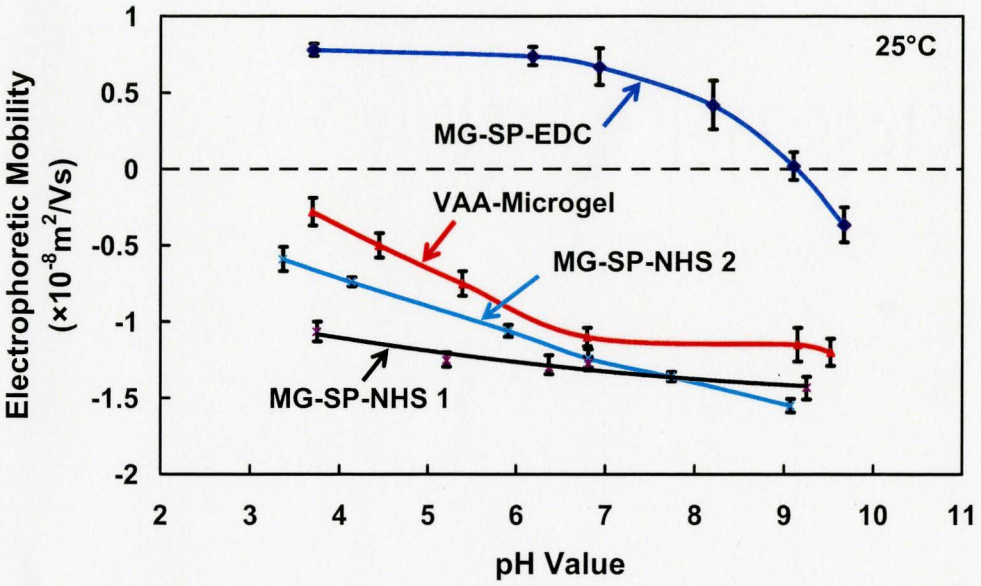

Figure 26: pH dependence of microgel, MG-SP-NHS 1, MG-SP-NHS 2 and MG-SP-EDC

Figure 26 shows the mobility response of different microgels as pH was varied. When microgel was treated with EDC and sulfo-NHS, then reacted with SP, the microgel became more negative, this is because the sulfo-NHS ester intermediates remain on the microgel surface, which has a SO_3^- group. When comparing the two methods of coupling SP to MG with EDC/NHS, it was found that MG-SP-NHS 2 has less negative charge, because MG-SP-NHS 2 reacted in higher pH (sodium phosphate buffer, pH= 7.4). The higher pH initiated a more active ester intermediate to react with SP.[55] This result is also confirmed in Figure 23, where MG-SP-NHS-2 had a higher SP concentration than MG-SP-NHS-1.

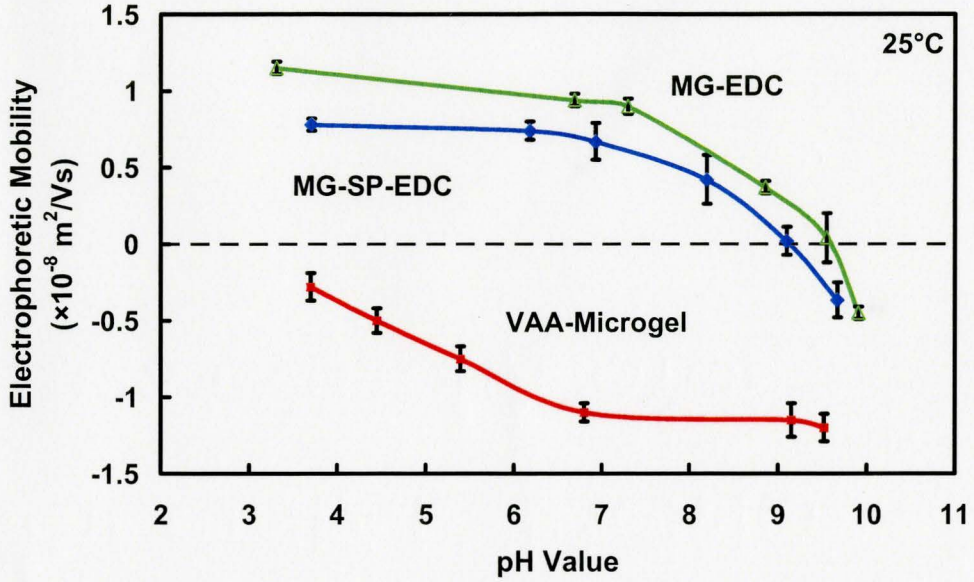

Figure 27: pH dependence of Mobility of VAA-Microgel, MG-SP-EDC and MG-EDC

Figure 27 illustrates the pH dependence of the electrophoretic mobility of VAA-Microgel, MG-SP-EDC, and MG-EDC. The SP treated microgel carries positive charge until pH 9, it is higher than its pI (6.5), which implies some active intermediate still exist in the system. Meanwhile, the control (MG-EDC), in which only VAA-Microgel reacted with EDC, carries higher positive charge compared to MG-SP-EDC, which confirms the presence of remaining positive intermediate on the microgel particle.

Nakajima et al. investigated the mechanism of amide formation by carbodiimide for bioconjugation in aqueous media (Figure 28). They proposed that the carbodiimide could react with amine or water molecules to yield amide bonds or carboxylate. In the

meantime, the carboxylic group could form a N-acylurea moiety, which is very stable in aqueous media,[77] when carbodiimide is present in excess. Swaisgood et al. also reported N-acylurea was formed when excess carbodiimide reacted with carboxylic groups.[78] This could be another explanation for the positive charge of MG-SP-EDC.

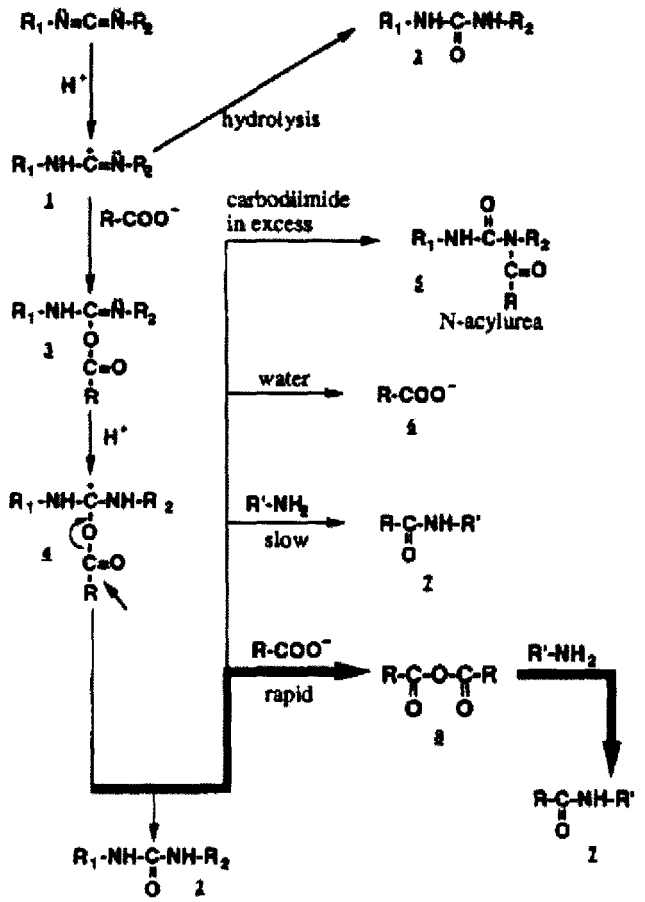

Figure 28: Proposed reaction mechanism of the amide formation between carboxylic acid and amine in aqueous media in the presence of carbodiimide (from refer 77)

4.6 Immobilize phage to microgel.

4.6.1 Immobilize biotin-phage to microgel.

Table 7: The number of active biotin-phage after immobilization

	Original phage (pfu/ml)	MG-Phage (pfu/ml)
1	1.1×10^{8}	4.0×10^{5}
2	1.1×10^{8}	3.5×10^{5}
3	2.45×10^{8}	6.8×10^{5}
Mean	$1.54\times10^{8} \pm 0.7$	$4.76\times10^{5} \pm 1.8$

4.6.2 Immobilize the T4 wild phage to microgel (control)

Table 8: The number of active T4 wild phage after immobilization

	Original phage	MG-phage
The concentration (pfu//ml)	1.3×10^{8}	$5.0\times10^{4} \pm 2.6$

The results in Table 7 and Table 8 indicated that both the biotin-phage and T4 wild phage can be immobilized on microgel particles, and the chemical attachment of biotin-phage to streptavidin-microgel particle resulted in a 10-fold improvement of attachment, compared with T4 wild phage. However, the fraction of phage binding to microgel was low, decreasing from 10^{8} to 10^{5} pfu/ml.

4.6.3 Calculation of the microgel/phage ratio.

Estimated concentration of active phage on microgel particles was calculated in Table 9.

Table 9: Calculation the concentration of phage on microgel particles

The number of phage:	
C_{phage}: = 4.76×10^{5} pfu/ml	Concentration of phage (pfu/ml)
V_{phage}: = 500 µl	Volume of phage
N_{phage}: = $C_{phage}\times V_{phage}$ = 2.4×10^{5}	Total number of phage
The number of microgel particles:	
D_{MG}: = 270 nm	Diameter of swollen microgel (nm)
SR: = D_{swell}/D_{dry} = 1.5	Swelling ratio from Figure 25
$D_{dry\ MG}$: = 180 nm	Diameter of microgel particle at pH 3 (nm)
$V_{dry\ MG} = \pi D^3/6 = 3.05\times10^{-3}$ $(\mu m)^3$	Volume of microgel particle at pH 3
ϕ_{pH3} = 85%	Volume fraction of PNIPAM at pH 3
Assume: ρ_{MG} = 0.9 mg/µl	Density of microgel particle
$M_{MG} = \rho_{MG}\times V_{dry}\times\phi_{pH3} = 2.34\times10^{-9}$ µg	Mass of microgel particle
C_{MG}: = 2 mg/ml	Concentration of microgel solution
V_{MG}: = 500 µl	Volume of the microgel solution
TM_{MG}: = $V_{MG}\times C_{MG}$ = 1 mg	Total mass of microgel particle
N_{MG}: = TM_{MG} / M_{MG} = 4.27×10^{11}	Total number of microgel particle
The microgel/phage ratio:	
N_{mg}/N_{phage}: = 1.78×10^{6}	The ratio of microgel/phage particle

Based on the results, there are 1.78 million microgels for every active biotin-phage, which indicates the microgel-phage coupling efficiency was very low. There are several possible reasons: Firstly, the SP distribution was not clear after the coupling reaction, and part of the SP could be denatured. It is possible that there could be more than one microgel particle bound to a single SP, thus leaving less binding sites for biotin-phage. Secondly, the number of biotin-phages immobilized on microgel could be much more, but most of them might have been deactivated after immobilization. The immobilization was performed in lambda buffer of pH 7.5. At

this condition, MG-SP-EDC still carries positive charge (Figure 27). Since the biotin-phage has a negative charge, the phage would attach to the MG-SP surface, and it will inhibit phage tails from reaching bacterial cells. Thirdly, Figure 27 shows that part of the intermediate, which may be N-acrylurea, still remains after the coupling reaction. It may also have influence on the SP and biotin-phage binding. Lastly, unlike the other small molecules, T4 biotin-phage particle has a relatively large size (200 nm long, 100 nm wide), which makes it hard to immobilize too much phage on a microgel particle and still maintain its infection.

4.7 Coat the microgel-supported phage to PAE/PVAm treated paper

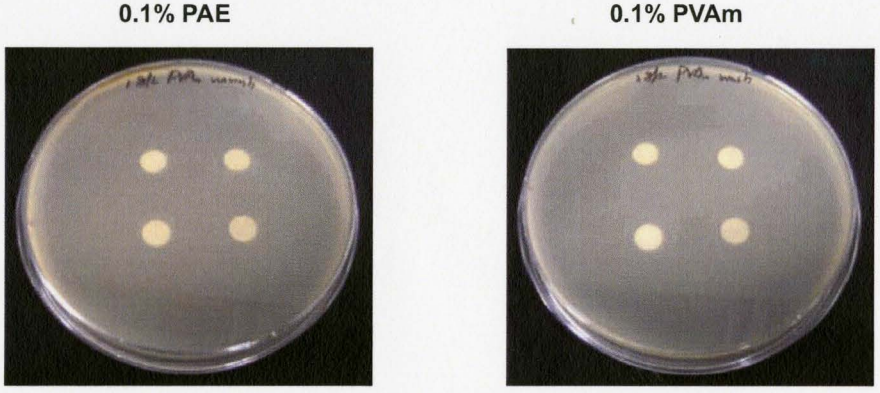

Figure 29: Phage infection from microgel-supported phage after washing.
(Left: 0.1% PAE treated paper; right: 0.1% PVAm treated paper)

The microgel supported phages were coated on PAE/PVAm treated paper as described before. Figure 29 shows that the microgel supported phage on PAE/PVAm paper still could not detect the bacteria because lysis did not appear, for which there

are also several possible reasons: The first reason is the low concentration of active biotin-phage on microgel as calculated before, there are roughly 10^6 microgels for every active phage, and former results in our group[79] showed microgel could penetrate into the paper through physical entrapment, which would inhibit the phage from detecting the bacterial cells. Second, the microgel-supported method was difficult to separate the negative charged phage from cationic PAE/PVAm treated paper, the phage particle could be easily absorbed onto the surface of positive charged paper through electrostatic interaction, and lost its infection. Generally, the microgel supported phage on modified paper surfaces was not a promising way of detecting bacteria.

Chapter 5: Conclusion

In this study, the negative charged biotin-phage was prepared with a measured size of 117 nm. Low phage adsorption and weak adhesion were displayed by unmodified filter paper because of electrostatic repulsion.

Compared with filter paper, PAE treated paper generated high phage binding efficiency and low phage activity due to the electrostatic interaction. Another cationic polymer PVAm exhibited strong phage adsorption and almost completely deactivated the phage particle. Phage was deactivated when coated to PVAm treated paper even before washing. Directly coating unsupported biotin-phage to wet strength resin treated paper was not a promising way for bioactive paper application, due to the phage deactivation.

VAA-Microgel particle was prepared for separating the biosensor (bacteriophage) from paper surfaces. Two different methods were used to couple Streptavidin to VAA-Microgel (MG-SP-EDC, and MG-SP-EDC-NHS). And more Streptavidin were coupled in MG-SP-EDC rather than MG-SP-EDC-NHS, resulted with SP coverage of 0.23 mg/m^2.

After coupling with EDC, the treated microgel showed a larger diameter than VAA-Microgel at low pH, increased from 180 nm to 235 nm, which indicated the coupling reaction generated a little aggregation. Mobility measurement confirmed that some intermediates remained on the microgel surface after the coupling reaction, which may due to the formation of N-acylurea moiety.

Biotin-phage could be immobilized to microgel particle and still carried infection. Chemical immobilization (Streptavidin-biotin) resulted in a 10-fold improvement of attachment when compared with T4 wild type phage.

The microgel-phage coupling efficiency was very low, there were more than 10^6 microgel particle for every active phage. And microgel supported phages were deactivated after coating to the PAE/PVAm treated paper.

Appendix:

Appendix 1: Calibration curve of Bradford assay

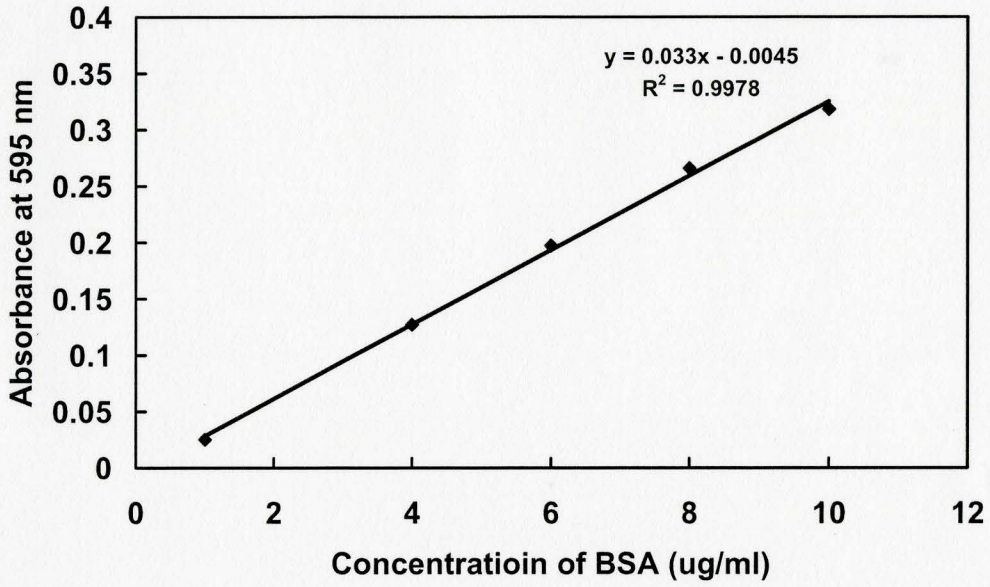

Figure 30: Calibration curve of Bradford micro assay using BSA in MES buffer

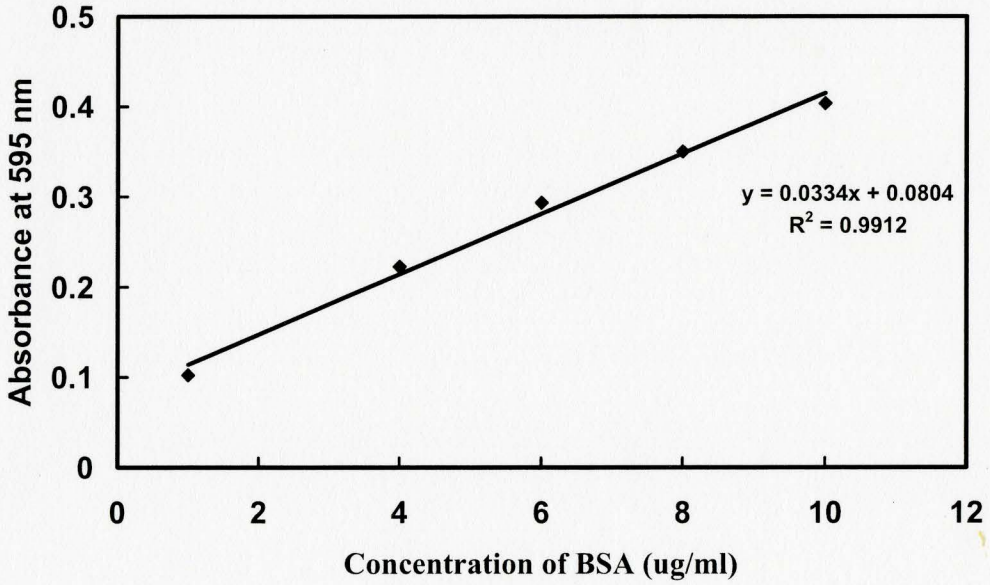

Figure 31: Calibration curve of Bradford micro assay using BSA in sodium phosphate buffer.

Appendix 2: Calculation of SP coverage

Mass of SP	
M_{SP}= 28.5- 8.3 μg = 20.2 μg	Mass of coupled SP
Number of microgel particles:	
$D_{dry\ MG}$: = 180 nm	Diameter of dry microgel particle at pH 3 (nm)
$V_{dry\ MG} = \pi D^3/6 = 3.05\times10^{-3}$ $(\mu m)^3$	Volume of single microgel particle
ϕ_{pH3} = 85%	Volume fraction of PNIPAM at pH 3
ρ_{MG} = 0.9 g/ml	Assuming density of microgel particle
$M_{MG}=\rho_{MG}\times V_{dry}\times \phi_{pH3}=2.34\times10^{-9}$ μg	Mass of microgel particle
TM_{MG}: = 2 mg	Total mass of microgel particle
N_{MG}: = TM_{MG} / M_{MG} = 8.54×10^{11}	Total number of microgel particle
$S= \pi D^2 = 1.02\times10^{-13}$ m^2	Surface area of single microgel particle
$TS=S\times N_{MG} = 8.71\times10^{-2}$ m^2	Total surface area of microgel
$\Gamma_{SP}= M_{SP}/TS$ = 0.23 mg/m^2	The ratio of microgel/phage particle

References:

1. **SENTINEL-The Bioactive Paper Network** www.bioactivepaper.ca **2005.**

2. **Diamond, D., *Principles of Chemical and Biological Sensors*. Wiley: New York, 1998; p 3.**

3. **VTT, Bioactive paper and fiber products** http://www.vtt.fi/**. 2006.**

4. **Henderson, D. A.; Inglesby, T. V.; Bartlett, J. G.; Ascher, M. S.; Eitzen, E.; Jahrling, P. B.; Hauer, J.; Layton, M.; McDade, J.; Osterholm, M. T., Smallpox as a Biological Weapon Medical and Public Health Management. In Am Med Assoc: 1999; Vol. 281, pp 2127-2137.**

5. **Janyapoon, K.; Korbsrisate, S.; Thamapa, H.; Thongmin, S.; Kanjanahareutai, S.; Wongpredee, N.; Sarasombath, S., Rapid Detection of Salmonella enterica Serovar Choleraesuis in Blood Cultures by a Dot Blot Enzyme-Linked Immunosorbent Assay. *Clinical and Vaccine Immunology* 2000, 7, (6), 977.**

6. **Mata, A. I.; Gibello, A.; Casamayor, A.; Blanco, M. M.; Dominguez, L.; Fernandez-Garayzabal, J. F., Multiplex PCR Assay for Detection of Bacterial Pathogens Associated with Warm-Water Streptococcosis in Fish. *Applied and Environmental Microbiology* 2004, 70, (5), 3183-3187.**

7. **Fratamico, P. M.; Strobaugh, T. P.; Medina, M. B.; Gehring, A. G., Detection of Escherichia coli 0157: H7 using a surface plasmon resonance biosensor. *Biotechnology Techniques* 1998, 12, (7), 571-576.**

8. **Petrenko, V. A.; Vodyanoy, V. J., Phage display for detection of biological threat agents. *Journal of Microbiological Methods* 2003, 53, (2), 253-262.**

9. **Smook, G. A., Handbook for Pulp & Paper Technologists. 1992. *Vancouver: Angus Wilde Publications*, 223-224.**

10. **Gervais, L.; Gel, M.; Allain, B.; Tolba, M.; Brovko, L.; Zourob, M.; Mandeville, R.; Griffiths, M.; Evoy, S., Immobilization of biotinylated bacteriophages on biosensors surfaces. *Sensors and Actuators B: Chemical* 2007, 125, (2), 615-621.**

11. Kutter, E.; Sulakvelidze, A., *Bacteriophages: Biology and Applications*. CRC Press: 2005.

12. Summers, W. C., How bacteriophage came to be used by the Phage Group. *Journal of the History of Biology* 1993, 26, (2), 255-267.

13. Merril, C. R.; Scholl, D.; Adhya, S. L., The prospect for bacteriophage therapy in Western medicine. *Nat Rev Drug Discov* 2003, 2, (6), 489-97.

14. Nakai, T.; Park, S. C., Bacteriophage therapy of infectious diseases in aquaculture. *Research in Microbiology* 2002, 153, (1), 13-18.

15. Bauman, R. W., Microbiology: Alternate Edition with Diseases by Body System. 2006, 189.

16. Kanamaru, S.; Leiman, P. G.; Kostyuchenko, V. A.; Chipman, P. R.; Mesyanzhinov, V. V.; Arisaka, F.; Rossmann, M. G., Structure of the cell-puncturing device of bacteriophage T4. *Nature* 2002, 415, (6871), 553-7.

17. Sun, W.; Brovko, L.; Griffiths, M., Use of bioluminescent Salmonella for assessing the efficiency of constructed phage-based biosorbent. *Journal of Industrial Microbiology and Biotechnology* 2001, 27, (2), 126-128.

18. Singleton, P., *Bacteria in Biology, Biotechnology and Medicine*. John Wiley and Sons: 2004.

19. Berg, H. C., *E. Coli in Motion*. Springer: 2003; p 1-6.

20. Espy, H. H., The mechanism of wet-strength development in paper: A review. *Tappi J* 1995, 78, (4), 90-99.

21. Chan, L. L., *Wet-strength resins and their application*. TAPPI Press: Atlanta, Ga. , 1994.

22. Espy, H. H.; Rave, T. W., The mechanism of wet-strength development by alkaline-curing amino polymer-epichlorohydrin resins. *Tappi journal* 1988, 71, (5), 133-137.

23. Roberts, J. C., *Paper Chemistry*. Chapman and Hall: 1991; p 82.

24. Feng, X.; Pouw, K.; Leung, V.; Pelton, R., Adhesion of Colloidal Polyelectrolyte Complexes to Wet Cellulose. *Biomacromolecules* 2007, 8, (7),

2161-2166.

25. Pelton, R.; Hong, J., Some properties of newsprint impregnated with polyvinylamine, Solutions! & TAPPI JOURNAL, December 2002, Vol. 1 (10)(147KB) Product Code: 02DEC21. *TAPPI JOURNAL* 2002, 1, (10).

26. Geffroy, C.; Labeau, M. P.; Wong, K.; Cabane, B.; Cohen Stuart, M. A., Kinetics of adsorption of polyvinylamine onto cellulose. *Colloids and Surfaces A: Physicochemical and Engineering Aspects* 2000, 172, (1-3), 47-56.

27. Pelton, R., Temperature-sensitive aqueous microgels. *Advances in Colloid and Interface Science* 2000, 85, (1), 1-33.

28. Hoare, T. Multi-responsive microgels: synthesis, characterization, and applications. McMaster University, Hamilton, 2006.

29. Nishiyama, Y.; Satoh, M., Collapse of a charged polymer gel induced by mixing "unfavorable" ounterions. *Polymer* 2001, 42, (8), 3919-3921.

30. Filipcsei, G.; Feher, J.; Zrinyi, M., Electric field sensitive neutral polymer gels. *Journal of Molecular Structure* 2000, 554, (1), 109-117.

31. Pelton, R. H.; Chibante, P., Preparation of aqueous lattices with N-isopropylacrylamide. *Colloids. Surf* 1986, 20, (3), 247-256.

32. Wu, J. Y.; Liu, S. Q.; Heng, P. W. S.; Yang, Y. Y., Evaluating proteins release from, and their interactions with, thermosensitive poly (N-isopropylacrylamide) hydrogels. *Journal of Controlled Release* 2005, 102, (2), 361-372.

33. Hoare, T.; Pelton, R., Functional group distributions in carboxylic acid containing poly (N-isopropylacrylamide) microgels. *Langmuir* 2004, 20, (6), 2123-33.

34. Kratz, K.; Hellweg, T.; Eimer, W., Influence of charge density on the swelling of colloidal poly (N-isopropylacrylamide-co-acrylic acid) microgels. *Colloids and Surfaces A: Physicochemical and Engineering Aspects* 2000, 170, (2-3), 137-149.

35. Dowding, P. J.; Vincent, B.; Williams, E., Preparation and Swelling Properties of Poly (NIPAM) "Minigel" Particles Prepared by Inverse Suspension Polymerization. *Journal of Colloid And Interface Science* 2000, 221, (2), 268-272.

36. Shibayama, M.; Tanaka, T.; Han, C. C., Small-angle neutron scattering study on weakly charged temperature sensitive polymer gels. *The Journal of Chemical Physics* 1992, 97, 6842.

37. Hoare, T.; Pelton, R., Highly pH and temperature responsive microgels functionalized with vinylacetic acid. *Macromolecules* 2004, 37, (7), 2544-2550.

38. Hoffman, A. S., Hydrogels for biomedical applications. *Advanced Drug Delivery Reviews* 2002, 54, (1), 3-12.

39. Hsu, F. Y.; Tsai, S. W.; Wang, F. F.; Wang, Y. J., The collagen-containing alginate/poly (L-lysine)/alginate microcapsules. *Artif Cells Blood Substit Immobil Biotechnol* 2000, 28, (2), 147-54.

40. Yoshioka, H.; Mikami, M.; Nakai, T.; Mori, Y., Preparation of poly(N-isopropylacrylamide)-grafted silica gel and its temperature-dependent interaction with proteins. *Polymer for Advanced Technologies* 1995, 6, (6), 418-420.

41. Ding, X. B.; Sun, Z. H.; Zhang, W. C.; Peng, Y. X.; Wan, G. X.; Jiang, Y. Y., Adsorption/desorption of protein on magnetic particles covered by thermosensitive polymers. *Journal of Applied Polymer Science* 2000, 77, (13), 2915-2920.

42. Cunliffe, D.; Alarcon, C. D.; Peters, V.; Smith, J. R.; Alexander, C., Thermoresponsive Surface-Grafted Poly (N-Isopropylacrylamide) Copolymers: Effect of Phase Transitions on Protein and Bacterial Attachment. *Langmuir* 2003, 19, (7), 2888-2899.

43. Kawaguchi, H.; Fujimoto, K.; Mizuhara, Y., Hydrogel microspheres III. Temperature-dependent adsorption of proteins on poly-N-isopropylacrylamide hydrogel microspheres. *Colloid & Polymer Science* 1992, 270, (1), 53-57.

44. Hoffman, A. S., Bioconjugates of Intelligent Polymers and Recognition Proteins for Use in Diagnostics and Affinity Separations. *Clinical Chemistry* 2000, 46, (9), 1478.

45. Silva, C. S. O.; Baptista, R. P.; Santos, A. M.; Martinho, J. M. G.; Cabral, J. M. S.; Taipa, M., Adsorption of human IgG on to poly (N-isopropylacrylamide)-based polymer particles. *Biotechnology Letters* 2006, 28, (24), 2019-2025.

46. Roque, A. C. A.; Taipa, M.; Lowe, C. R., An artificial protein L for the purification of immunoglobulins and Fab fragments by affinity chromatography. *Journal of Chromatography A* 2005, 1064, (2), 157-167.

47. Nolan, C. M.; Serpe, M. J.; Lyon, L. A., Thermally modulated insulin release from microgel thin films. *Biomacromolecules* 2004, 5, (5), 1940-1946.

48. Nayak, S.; Lee, H.; Chmielewski, J.; Lyon, L. A., Folate-mediated cell targeting and cytotoxicity using thermoresponsive microgels. *J. Am. Chem. Soc* 2004, 126, (33), 10258?0259.

49. Hu, Z.; Chen, Y.; Wang, C.; Zheng, Y.; Li, Y., Polymer gels with engineered environmentally responsive surface patterns. *Nature(London)* 1998, 393, (6681), 149-152.

50. Eakin, R. E.; Snell, E. E.; Williams, R. J., THE CONCENTRATION AND ASSAY OF AVIDIN, THE INJURY-PRODUCING PROTEIN IN RAW EGG WHITE. *Journal of Biological Chemistry* 1941, 140, (2), 535-543.

51. Diamandis, E. P.; Christopoulos, T. K., The biotin-(strept) avidin system: principles and applications in biotechnology. *Clin. Chem* 1991, 37, (5), 625-636.

52. Savage, M. D., *Avidin-biotin Chemistry: A Handbook*. Pierce chemical company: 1992.

53. Smith, C. L.; Milea, J. S.; Nguyen, G. H., Immobilization of Nucleic Acids Using Biotin-Strept(avidin) Systems. *Topics in Current Chemistry* 2006, 261, 63-90.

54. Chen, L.; Schechter, B.; Arnon, R.; Wilchek, M., Tissue selective affinity targeting using the avidin-biotin system. *Drug Development Research* 2000, 50, (3-4), 258-271.

55. Hermanson, G. T., Bioconjugate Techniques. 1996. In Academic Press, New York.

56. Donovan, J. A.; Jennings, M. L., N-hydroxysulfosuccinimido active esters and the L-(+)-lactate transport protein in rabbit erythrocytes. *Biochemistry* 1986, 25, (7), 1538-1545.

57. EDC, PIERCE biotechnology. http://www.piercenet.com/.

58. Staros, J. V.; Kakkad, B. P., Cross-linking and chymotryptic digestion of the extractoplasmic domain of the anion exchange channel in intact human erythrocytes. *Journal of Membrane Biology* 1983, 74, (3), 247-254.

59. Debord, J. D.; Lyon, L. A., On the Unusual Stability of Succinimidyl Esters in pNIPAm-AAc Microgels. *Bioconjugate Chem* 2007, 18, (2), 601-604.

60. Su, S.; Ali, M. M.; Filipe, C. D. M.; Li, Y.; Pelton, R., Microgel-Based Inks for Paper-Supported Biosensing Applications. *Biomacromolecules* 2008.

61. Bradford, M. M., A rapid and sensitive method for the quantitation of microgram quantities of protein utilizing the principle of protein-dye binding. *Anal Biochem* 1976, 72, (1-2), 248-254.

62. Compton, S. J.; Jones, C. G., Mechanism of dye response and interference in the Bradford protein assay. *Analytical biochemistry* 1985, 151, (2), 369-374.

63. Sedmak, J. J.; Grossberg, S. E., A rapid, sensitive, and versatile assay for protein using Coomassie brilliant blue G250. *Anal Biochem* 1977, 79, (1-2), 544-52.

64. Wheat, P. F., History and development of antimicrobial susceptibility testing methodology. In Br Soc Antimicrob Chemo: 2001; Vol. 48, pp 1-4.

65. Heatley, N. G., A method for the assay of penicillin. *Biochemical Journal* 1944, 38, 61-5.

66. Bauer, A. W.; Kirby, W. M.; Sherris, J. C.; Turck, M., Antibiotic susceptibility testing by a standardized single disk method. *Am J Clin Pathol* 1966, 45, (4), 493-6.

67. Rolinson, G. N.; Russell, E. J., New Method for Antibiotic Susceptibility Testing. *Antimicrobial Agents and Chemotherapy* 1972, 2, (2), 51-56.

68. NCCLS-19:21, National Committee for clinical laboratory standards. Performance standards for antimicrobial susceptibility testing: ninth informational supplement. In 1999.

69. Tolba, M.; Brovko, L.; Griffiths, M., Bacteriophage-modified paper that kills *Escherichis coli*. In Personal communication: 2006.

70. Krueger, A. P.; Ritter, R. C.; Smith, S. P., The electrical charge of

bacteriophage. *JEM* 1929, 50, 739-746.

71. Clifton, C. E.; Madison, R. R., Studies on the electrical charge of bacteriophage. *J. Bacteriol.* 1931, 22, (4), 255-260.

72. Yamaguchi, Y.; Yanagida, M., Head shell protein hoc alters the surface charge of bacteriophage T4. Composite slab gel electrophoresis of phage T4 and related particles. *J Mol Biol* 1980, 141, (2), 175-93.

73. Childs, J. D., Effect of hoc protein on the electrophoretic mobility of intact bacteriophage T4D particles in polyacrylamide gel electrophoresis. *J. Mol. Biol.* 1980, 141, 163-173.

74. Dabrowska, K.; Zembala, M.; Boratynski, J.; Switala-Jelen, K.; Wietrzyk, J.; Opolski, A.; Szczaurska, K.; Kujawa, M.; Godlewska, J.; Gorski, A., Hoc protein regulates the biological effects of T4 phage in mammals. *Archives of Microbiology* 2007, 187, (6), 489-498.

75. Sirotkin, A. K.; Sukhinin, V. P.; Nazarova, O. V.; Gavrilova, I. I., Synthetic Polymers in Studies on the Adsorption of Viral Particles. *Doklady Biochemistry and Biophysics* 2003, 388, 60-63.

76. Huang, S. C.; Swerdlow, H.; Caldwell, K. D., Binding of biotinylated DNA to streptavidin-coated polystyrene latex. *Anal Biochem* 1994, 222, (2), 441-9.

77. Nakajima, N.; Ikada, Y., Mechanism of Amide Formation by Carbodiimide for Bioconjugation in Aqueous Media. *Bioconjugate Chemistry* 1995, 6, (1), 123-130.

78. Swaisgood, H.; Natake, M., Effect of Carboxyl Group Modification on Some of the Enzymatic Properties of L-Glutamate Dehydrogenase. *Journal of Biochemistry* 1973, 74, (1), 77.

79. Su, S. Biomacromolecules in paper for strength and bio-detection. McMaster University, Hamilton, Ontario, 2007.